Focused R&D for Electrochromic Smart Windows: Significant Performance and Yield Enhancements

Continuation Application

Type of Report:	Topical
Reporting Period Start Date:	September 30, 2001
Reporting Period End Date:	January 31, 2003
Principal Authors:	Dr. Mark Burdis Dr. Neil Sbar
Date Report was Issued:	November 30, 2002
DOE Award Number:	DE-FC26-01NT41259
Submitting Organization:	SAGE Electrochromics, Inc 2150 Airport Drive Faribault, MN 55021 507-333-0078 www.sage-ec.com

I. INTRODUCTION AND SUMMARY

DESCRIPTION AND BENEFITS OF ELECTROCHROMIC WINDOWS

There is a need to improve the energy efficiency of building envelopes as they are the primary factor governing the heating, cooling, lighting and ventilation requirements of buildings – influencing 53% of building energy use. In particular, windows contribute significantly to the overall energy performance of building envelopes, thus there is a need to develop advanced energy efficient window and glazing systems.

Electrochromic (EC) windows represent the next generation of advanced glazing technology that will (1) reduce the energy consumed in buildings, (2) improve the overall comfort of the building occupants, and (3) improve the thermal performance of the building envelope. "Switchable" EC windows provide, on demand, dynamic control of visible light, solar heat gain, and glare without blocking the view. As exterior light levels change, the window's performance can be electronically adjusted to suit conditions. A schematic illustrating how SageGlass® electrochromic windows work is shown in Figure I.1.

SageGlass® EC glazings offer the potential to save cooling and lighting costs, with the added benefit of improving thermal and visual comfort. Control over solar heat gain will also result in the use of smaller HVAC equipment.

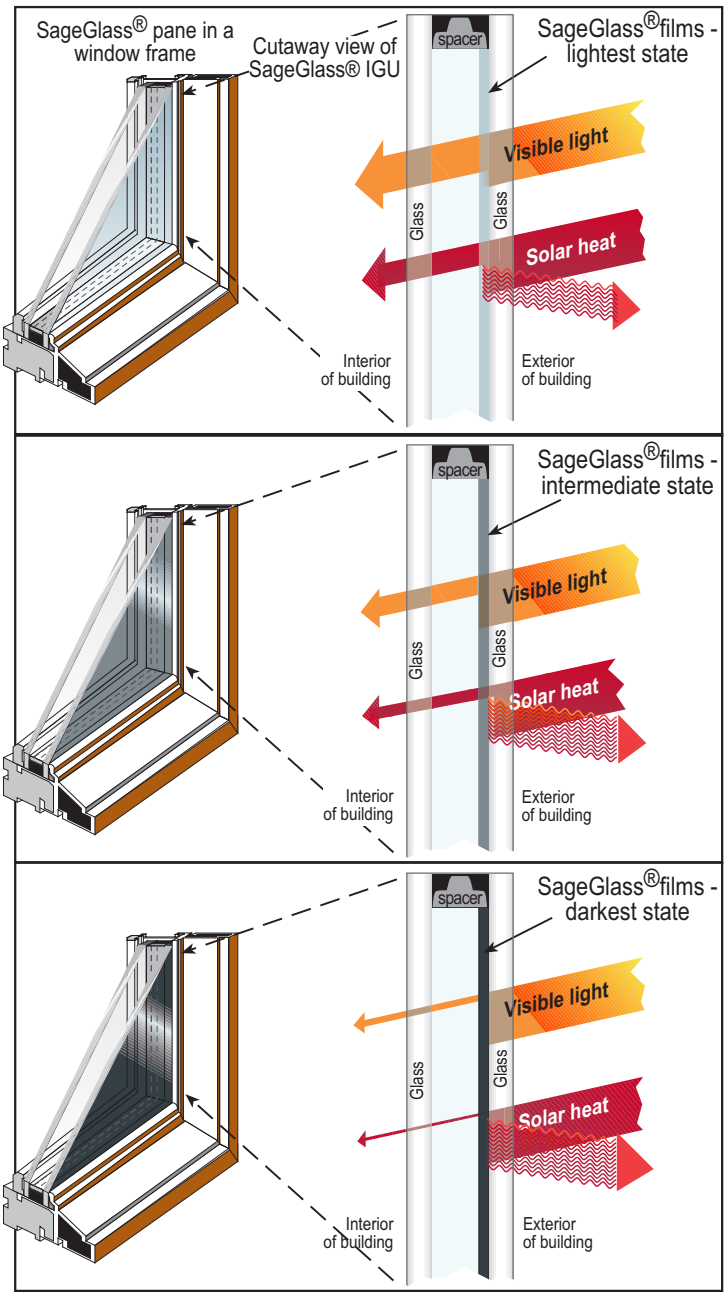

Figure I.1 – Schematic of the principle of operation of a SageGlass® EC window.

If a step change in the energy efficiency and

performance of buildings is to be achieved, there is a clear need to bring EC technology to the marketplace. This project addresses accelerating the widespread introduction of EC windows in buildings and thus maximizing total energy savings in the U.S. and worldwide.

We report on R&D activities to improve the optical performance needed to broadly penetrate the full range of architectural markets. Also, processing enhancements have been implemented to reduce manufacturing costs. Finally, tests are being conducted to demonstrate the durability of the EC device and the dual pane insulating glass unit (IGU) to be at least equal to that of conventional windows.

EC WINDOW TECHNOLOGY

The SAGE EC device is a series of thin films deposited onto a glass substrate one on top of the other to form a stack. This is shown in Figure I.2. The outermost layers are transparent conductors, which are used to apply a voltage to the active layers that are sandwiched between. The active layers consist of a WO_3 electrochromic (EC) layer, an ion conductor (IC) layer, and a counter electrode layer (CE). Charge, in the form of electrons and ions, is shuttled between the CE and the EC layers, producing the bleached and colored states respectively: The electrons are passed around the outer circuit, while the ions are transported through the IC. Insertion of charge into the EC layer will cause that layer to color to a depth which depends upon the amount of charge transferred. The effect is completely reversible, and is accomplished simply by reversing the polarity of the voltage. This is shown schematically in Figure I.2.

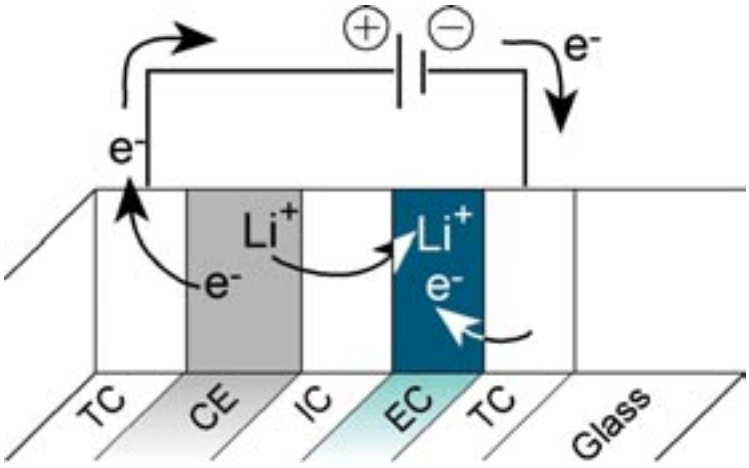

Figure I.2 – The SageGlass® electrochromic device.

BUDGET PERIOD I WORKPLAN ACTIVITIES

Materials Developments*:* Each of the active EC layers was optimized with respect to device optical performance and processibility. The basic approach to evaluating each alternative sputtered material and/or composition includes fabricating a small sputtering target for use on our laboratory MRC coaters. Films are deposited and analyzed using

a variety of techniques with support from The Center for Interfacial Engineering at the University of Minnesota. Experiments on solution deposited films were performed with help from the Center for Microengineered Materials at the University of New Mexico (Brinker group). Work was carried out to determine the impact of materials properties on the color of the device, with the goal of achieving better color neutrality. We additionally focused on materials and process changes to increase dynamic range and optimize switching performance. If desirable film properties can then be achieved on a lab scale, full size pilot line targets and processing will be implemented for the production of large area windows.

Device Modeling: A solid-state model was developed to explore the electronic behavior of SageGlass® devices. We have found that good devices have a leakage characteristic similar to that of a diode. The current work is focused on understanding the contributions of the various device layers and interfaces to this diode effect. The goal is to enable maximum coloring current before the electronic leakage limits the dark state optical density.

Process Improvement: The objective of this activity is to optimize processing parameters to achieve the best device performance. However, device fabrication through pilot line coating operations is a multivariate process and, the variables are not always independent (interactions can become important). Consequently, we have implemented Design of Experiments (DOE) techniques to identify the key processing variables, among the multiple fabrication steps, that have the most impact on performance, yields and throughput. Initial process optimizations have been carried out, with encouraging results.

Operational Testing*:* Operational testing refers to post-manufacturing device testing to determine through optical and electrical measurements whether the EC glazing meets product specifications. Over the last 12 months, requirements and test parameters have been defined and a prototype test station has been built and evaluated. We are able to measure and record the key performance characteristics. A second aspect of this task involves achieving a better understanding of voltage/current relationships so that initial dynamic measurements of device performance can be used to predict final steady state properties. This is a complex problem; however, initial work to understand the equivalent device circuit has yielded promising results.

IGU Durability and Integrity: The IGU seal must remain a moisture barrier over the lifetime of the window. SAGE has partnered with the industry leading IGU fabricator to produce durable IGU products to develop and exhaustively test EC IGUs. The first task was to develop a low-cost interconnection system for bringing power through the sealing system to the EC device. This system must resist corrosion and not compromise the moisture barrier properties of the primary seal. The second task was to develop and implement a series of tests to measure the durability of the EC IGU. Accelerated tests included the aggressive P1 test, temperature cycling, humidity aging, low temperature testing, and thermal shock. The SAGE EC fabrication and sealing system proved to be remarkably robust with respect to the above high stress conditions.

II MATERIALS DEVELOPMENT

II.1 WO_3 IMPROVEMENTS

To improve both the performance and marketability of our SageGlass® products, one of the main issues is the color of the device, both in the fully darkened and bleached states. Currently, the bleached state coloration contains a small degree of absorption, which is manifested as a slight yellow tinge, and the colored state color is slightly blue-gray. It is highly desirable to reduce the coloration in the bleached state, and to shift the dark state color more towards neutral.

The color of an EC device is a complex function of the different layers of which it is composed. To be capable of predicting the color of an EC device, it is necessary to understand each layer individually, as well as to know how the layers interact with each other. In the case of SAGE's EC device, intimate knowledge is needed of the optical properties for the five basic EC layers—two transparent conductors, an electrochromic layer, an electrolyte, and a counter-electrode layer—plus whichever optical matching layers may be present. Furthermore, it is necessary to have a good understanding of the way they interact optically.

Work associated with the WO_3 carried out during this project is specifically targeted toward modification of the optical properties of that layer to produce improved coloration in the *dark* state, as this is the layer which contributes most to the blue coloration in that state.

Several other research groups[1] have studied the doping of WO_3 with various other elements to shift the absorption band—centered in the near infra-red in pure WO_3—more into the visible to produce a more acceptable looking colored state. The most commonly studied dopant is Mo, although several others have been used.[2],[3] The accepted model suggests that optical transitions, while possible between W^{5+} and W^{6+} states in pure WO_3, are also possible between Mo^{5+} and Mo^{6+}, and Mo^{5+} and W^{6+} depending on the concentration of Mo atoms and the total amount of inserted Li. The proposed mechanism is for the electrons associated with the inserted lithium to initially occupy lower energy sites associated with the Mo ions, from where transitions to empty Mo or W sites are then possible. (Note: This class of electrochromic materials colors by a mechanism called intervalence charge transfer. This involves an electron initially reducing one of the ions in the host lattice, and then 'hopping' to a nearby 'empty' ion.) The occupation of the Mo sites upon further addition of lithium continues until all the Mo sites are occupied, whereupon occupation of the W sites commences, leading to possible transitions between W^{5+} and W^{6+} sites, giving a much more distributed absorption and hence a more neutral coloration. Further credence is given to this model by a successful application to a completely different mixed oxide system, that of $V_xTi_{1-x}O_y$.[4]

[1] See for example C.G.Granqvist, 'Handbook of Inorganic Electrochromic Materials', Elsevier (1995) Chapter 13 p225
[2] Faughnan and Crandall, Appl. Phys. Lett. **31**, 834-836 (1977).
[3] Yamada and Kitao, SPIE Vol **IS4** pp246-259, (1990).
[4] Burdis, Thin Solid Films, **311** (1997) 286-298

II.1.1 Doped tungsten target

A Mo (10wt%) doped W target was obtained for our lab coater. Thin films were deposited onto both plain glass and tin oxide coated substrates to make both electrochemical and optical measurements. The overall aim was to determine whether the W:Mo mixed oxide would provide better neutrality for the finished device, without compromising the electrochemical performance.

Thin films were deposited from the mixed metal target, and the optical properties evaluated in the usual way. It was found that the sputtering process from the doped target was not very different from the pure W target. This meant that we were able to deposit transparent films fairly quickly. Indeed, the refractive index for the mixed metal oxides was also within the range of those obtained from pure WO_3.

The electrochemistry of the mixed W:MoO_x films was found to be acceptable, and once again, indistinguishable from the electrochemistry expected from WO_3 films. However, it was noted that the coloration for the mixed metal films displayed a more neutral coloration for the initial stages of coloration (i.e. from around 70% down to 25%), than an equivalent thickness WO_3 film. It was also noted that the film became rapidly more blue as coloration proceeded, and was almost indistinguishable from the WO_3 film when fully colored. It would be of interest to obtain a target with a higher degree of Mo doping, and repeat this work to determine whether it is possible to maintain the neutrality throughout the full coloration range.

II.1.2 WO_3 film structure and processing to control and minimize blind charge

There have been many references in the open literature to a phenomenon that we refer to as “blindcharge.” This is the irreversibly incorporated lithium which is not recovered from the WO_3 film after the first color-bleach cycle, however it causes no coloration in the WO_3 and does not seem to upset the electrochemical kinetics of the insertion process. From this perspective, it does not appear to be a problem, but in fact, variable loss of lithium from the EC device during switching makes it difficult to precisely determine the lithium titration needed for optimum dynamic range. It is clearly important to control the amount of blindcharge resident in the as-deposited WO_3 films. Two methods for doing so are discussed below: (i) deposition of WO_3 from a ceramic target, and (ii) deposition of WO_3 in the transition region of the sputtering characteristic.

II.1.3 Thin film deposition from a WO_3 target

As we have mentioned previously, the current SageGlass® process uses a WO_3 thin film as the electrochromic layer. This is deposited at elevated temperatures by a reactive magnetron sputtering process. This heating process is required to be highly uniform, is time consuming and therefore expensive to implement in a high throughput manufacturing operation. There are several drawbacks to this heating step: (1) It consumes a great deal of energy; (2) it requires time to both heat up and cool down the glass, leading to a reduction in the potential throughput of the manufacturing facility; (3) it places very stringent requirements on the uniformity of heating over the entire area of

the glass, any loss of which can lead to a reduction in the yield; (4) it forces a section of the sputtering plant to be devoted to heating, and therefore increases capital cost, as well as the area of the sputtering machine; (5) it requires some device to act as a heat reservoir to maintain the high temperature of the glass during deposition of the layer—currently we use a large metal backing plate, which takes time to heat up and is subject to warping and consequently may lead to non-uniform heating; and (6) it can cause detempering of the tempered glass required for certain applications. In addition, handling large pieces of hot glass adds an additional hazard for the operator to an already difficult process.

An elegant solution to these two problems would be to eliminate the need for heating altogether. This has been shown to be possible by using a ceramic target[5], and experiments in our lab have shown that WO_3 films with acceptable electrochromic properties can be deposited from a ceramic target using DC magnetron sputtering.

To understand the motivation for using a ceramic target in the first place, it is necessary to briefly consider some of the properties of the WO_3 films. We use four main measurements to characterize the single layers of WO_3: (1) the thickness, (2) the transmission and reflection characteristics (and therefore the optical constants), (3) the electrochromic efficiency, and (4) the amount of irreversibly incorporated charge held in the film after cycling (the blindcharge). We now consider each of these properties briefly, and compare the behavior of films deposited from our pilot line and the ceramic target in the lab coater:

Thickness: It is well known that the optical absorption of WO_3 films in the colored state obeys the Beer-Lambert law up to a point where the absorption saturates. We see therefore that the dark state coloration will ultimately be limited by the thickness of the WO_3, and so it is necessary to deposit a thick enough layer to give an acceptable dark state transmission. This only really becomes important when we consider a manufacturing operation, where throughput becomes important, and so film deposition rate becomes critical to achieving economical production. During our study of deposition from the ceramic target, it was found that the deposition rates for DC magnetron sputtered WO_3 were comparable if not higher than for films sputtered in the same sputtering system but from a metal target.

Transmission: The transmission of an EC device in the clear state will be an amalgamation of the optical properties of all of the individual layers making up the stack. It is possible to design a layer structure that can take advantage of the differences in refractive indices to boost the transmission of the overall stack for non-absorbing films. However any absorption in any of the layers will reduce the overall transmission in the clear state, thus reducing the dynamic range of the EC device. Highly transparent films of WO_3 were deposited from the ceramic target during this work. An example is shown in Figure II.1 in the Appendix.

Electrochromic Efficiency: The electrochromic efficiency η, of the film is defined as the change in optical density per unit charge inserted,

[5] M.S.Burdis and J.R.Siddle, Thin Solid Films, 237 (1994) 320-325

$$\eta = OD/\rho$$

and the optical density is given by

$$OD = \log (T(\rho)/T_o)$$

Where $T(\rho)$ is the transmission for an inserted charge density of ρ, and T_o is the initial transmission. Once again, the measurements of electrochromic efficiency for the films deposited from the ceramic target compared favorably with those from the standard process.

Blindcharge: The blindcharge is measured by cycling the film in a lithium-containing electrolyte (wet cell) and then carefully measuring the current flowing into and out of the film. Invariably, the amount of charge inserted into the film will exceed the amount extracted, and this unrecovered charge is referred to as blindcharge. (It is "blind" as it causes no coloration of the film.) It was thought that the blindcharge would cause a problem later in the process, as the net amount of lithium remaining in the device after the lithiation process would be a simple sum of the amount inserted less the amount removed by satisfying the blindcharge on the first cycle. We have clear evidence that this will lead to a device that will lose several percent in transmission after the first color-bleach cycle. It would therefore seem sensible to try to minimize the amount of blindcharge present in the film, and indeed, this is the reason for depositing the WO_3 onto a heated substrate. The amount of blindcharge also depends on the amount of oxygen in the sputtering environment. Films were deposited from the ceramic target to try to achieve comparable electrochromic properties. The deposition parameters and some measured properties are given in Table II.1 in the Appendix.

The majority of these films have good transparency, adequate EC efficiency, acceptable thickness and lower blindcharge than the typical pilot line samples. In fact, these films were deposited at a rate equivalent to, or higher than that seen by reactive DC magnetron sputtering from a metal target in the same system. However, there was one issue with these films: The reversibility of the charge insertion (in this case the charge which caused coloration, not the blindcharge) seemed to get worse as gas mixture was changed. Thus there was a trade-off between the reversibility and the amount of blindcharge. A set of deposition conditions was selected, which ensured good reversibility. The amount of blindcharge was still less than contained in the standard pilot line samples. Films were therefore deposited onto the substrate to make complete devices.

Several 5.5" x 6" samples of WO_3 were prepared with the ceramic target under normal sputtering conditions on the lab coater. These nominally identical samples have low blindcharge, good electrochromic efficiency, and normal thickness, which is similar to the pilot line WO_3. These samples comprised set A.

One set of samples (set B) was processed, also with the ceramic target, with one slightly different parameter, which yielded a film with some absorption. The transmission of this film was around 55%. Generally, WO_3 a SnO_2 covered substrate has significantly higher transmission.

Three samples from set A and one from set B were processed into full devices alongside a pilot line sample (substrate label L6-64) using our standard processing conditions. The results are presented in Table II.2 (Appendix).

The sample from set B that was initially sub-stoichiometric—i.e. blue after WO_3 deposition—cleared up during subsequent heat treatments. This indicates an insertion of oxygen into the WO_3 during this process. This could be from the oxygen in the firing atmosphere.

Table II.3 (Appendix) shows the switching performance of the samples.

Each sample except 802A (WO_3 deposited on the pilot line in the usual way) had several shorts that were very difficult to "blow," and appeared to be very leaky electronically. This means that application of the voltage drives an electronic current, which effectively shorts out the ionic current, leading to reduced (or sometimes no) coloration. Application of higher voltages caused the windows to color much darker (802C went to 23% at 9V). The color was very neutral gray where they did switch, however, these devices obviously do not meet our process specification limits.

The switching performance of the EC devices with WO_3 deposited from the ceramic target is very poor when compared with pilot line devices. It is difficult to understand why samples should behave this way given the promising results we obtained in the wet-cell. However, we cannot rule out the possibility that the redistribution of lithium from the other layers is different for the samples prepared with WO_3 from the ceramic target, when compared with "normal" WO_3. We suspect that the electronic leakage of EC devices depends strongly on the level of lithium, and a difference in WO_3 preparation may lead to a difference in the electrochemical potentials throughout the device, and hence the different leakage behavior.

Several other attempts have been made to try to produce devices with the WO_3 deposited from the ceramic target, but all have produced the same result where the samples are extremely electronically leaky, while the control samples behave normally. We are forced to conclude that there is an interaction between the IC (which we assume dominates the electronic behavior of the device) and the underlying WO_3. We have decided to investigate the nature of these interactions prior to proceeding with any of the tasks associated with the ceramic target.

Cold Reactive WO_3 deposition

As we have already seen, additional heating is required for the current WO_3 deposition process. This has implications of great capital cost in the upcoming production facility, as well as causing problems in obtaining repeatable and uniform glass temperature. We have produced WO_3 films that perform reasonably well in a wet-cell evaluation when deposited in the transition region between the oxide and metallic modes. Figure II.2 (Appendix) shows the measured hysteresis curve for our pilot line WO_3 process.

These data are obtained by running the target at a fixed power and pressure and measuring the voltage as the gas flows are varied in a controlled manner. Beginning with an oxygen rich environment, the argon level is gradually increased, and the pressure maintained constant by automatically controlling the oxygen flow. This process is continued until the target flips metallic (indicated by a sharp increase in the voltage), and then the process is reversed and the argon flow is reduced.

Our normal pilot line process is run far out in the oxide region onto a heated glass substrate. For this study, we ran WO_3 samples at various points on the hysteresis curve, but with no substrate heating, and evaluated their electrochromic properties by the usual wet-cell techniques. It was found that there is residual absorption in these films if they are run at too high a voltage, (i.e. close to the metallic regime) but very acceptable properties can be obtained for films run in the transition region.

A run of four complete EC devices was made, where the only deviation from our standard process was to deposit the WO_3 in the transition region with *no substrate heating*. All devices were initially greenish-gray. In the colored state, they were neutral at one edge and faded to brown at the opposite side. After cycling, the color was brown. This is summarized in Table II.4 (Appendix):

There is a significant loss of transmission upon cycling, but this is probably due to there being a small amount of residual blindcharge, and could be addressed by increasing the amount of lithium inserted into the device. We also noted that the devices were somewhat electronically leaky, suggesting once again that the nature of the WO_3 is important to determining the electronic properties of the device. However, the devices switched fairly well, coloring to around 10% in each case. The variation is most likely due to an unintentional variation in the level of lithium, due to a non-uniformity that we were experiencing at the time of these experiments.

In summary, depositing WO_3 in transition mode shows promise for eliminating (or greatly reducing) the need for pre-heating the WO_3. The reduction of the bleached-state transmission after cycling indicates that there is still excessive blind-charge in the WO_3, and once again, this should be easy to rectify by adjusting the amount of lithium inserted into the device. In addition to saving heating time, this process variation shows the potential to cut deposition time by 75% because the deposition rate is 4X that of the standard process. This also means that the capital requirements for cathodes, power supplies, pumps and flow controllers for a production coater would be significantly reduced.

II.1.4 Role of defects on electrochromic properties

We are currently studying the role of defects (contamination and chemical/structural inhomogeneities) on the performance of SAGE electrochromic devices using a combination of surface analytical techniques including SEM, XPS, ESCA, SIMS, TEM and AAS. The overall goal is to characterize these defects and understand their effects on electro-optical properties, identify and eliminate the defect source, or if this is impossible or impractical (*e.g.*

material defects introduced from external suppliers), to modify our fabrication process to render the defects benign. We will limit the current discussion to two main areas: (i) defects that create localized non-coloring regions (ranging in size from 100 to 750 microns in diameter); and (ii) defects that affect the local switching potential by creating shorts. Although several of the analysis techniques are used to investigate the defects, we present only some of the SEM and SIMS images here.

Non-coloring defects

The most common defects that cause non-coloring areas arise either from surface chemical impurities or cracks in the transparent electronic conductor layer on the glass substrate. Chemical impurities include NaCl, which forms as a reaction between the sodium in the glass substrate and chlorinated reactants of the tin oxide CVD process.[6] The NaCl crystals can be large on the scale of electrochromic film thicknesses (photomicrograph 1) and lead to perturbations in the film structure. Since these crystals are water-soluble, they often leave behind large voids in the transparent conductor film (photomicrograph 2) that also interfere with the electrochromic film structure. Careful substrate cleaning to remove these impurities prior to film deposition is critical and as a direct result of this work, we have begun a thorough review of our cleaning and tempering processes, with encouraging results.

Cracks in the transparent conductor (TC) layer, formed either during substrate manufacture, or film deposition/heat treatment can also lead to migration of species (notably sodium) from the underlying glass into the electrochromic film stack and affect local film optical properties. These cracks can be small (on the order of a few microns), yet create large non-coloring regions. Photomicrograph 3 shows a non-coloring area viewed using SEM and a sodium map using secondary ion mass spectroscopy (SIMS). In this case, the TC defect (crack) responsible for a non-coloring area is approximately two orders of magnitude smaller than the optical defect size. The SIMS investigation shows correlation between the size of the non-coloring area and the Na zone around the TC defect. Efforts are underway to modify our process to (i) minimize the crack formation during processing, and (ii) decrease the migration of chemical species from the substrate and hence moderate their influence on film chemistry.

Localized shorting defects

There are a number of defect types that may cause an electrical short-circuit during device coloring, and can be categorized as either substrate-induced, or process-induced. Defects caused by substrate manufacturing include TC rubble or Sn specks (photomicrograph 4). Process-induced defects can be generated by improper cleaning (residual particles or glass chips can be ground into the TC surface during cleaning), contamination during bus bar application (Pphotomicrograph 5), and defects formed during the film deposition process. Arcing from the target or substrate carriers can sometimes form “droplet”-like defects (photomicrograph 6) during sputter deposition. Current efforts are focused on improving substrate cleaning and minimizing process-induced defect formation.

[6] (See, for example, Allendorf, M.D. “On-line Deposition of Oxides on Flat Glass” in *Interface*, Summer 2001, pp. 34-48. The Electrochemical Society)

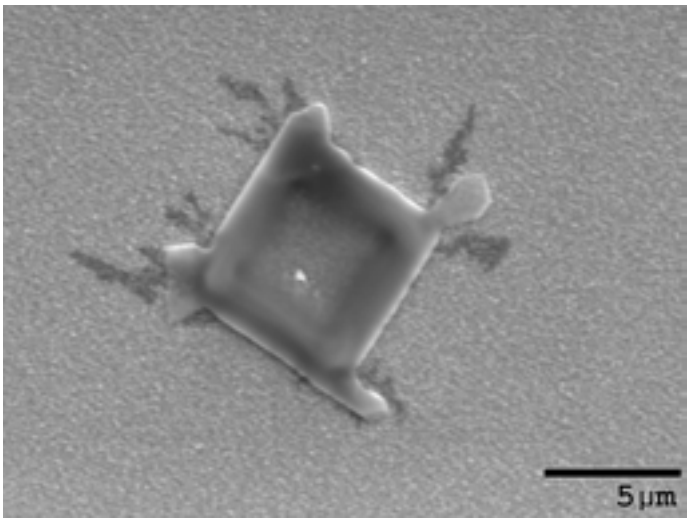

Photomicrograph 1 – SE image of NaCl crystal on a TC coated substrate. A dark Na phase is also visible at the corners of the crystal.

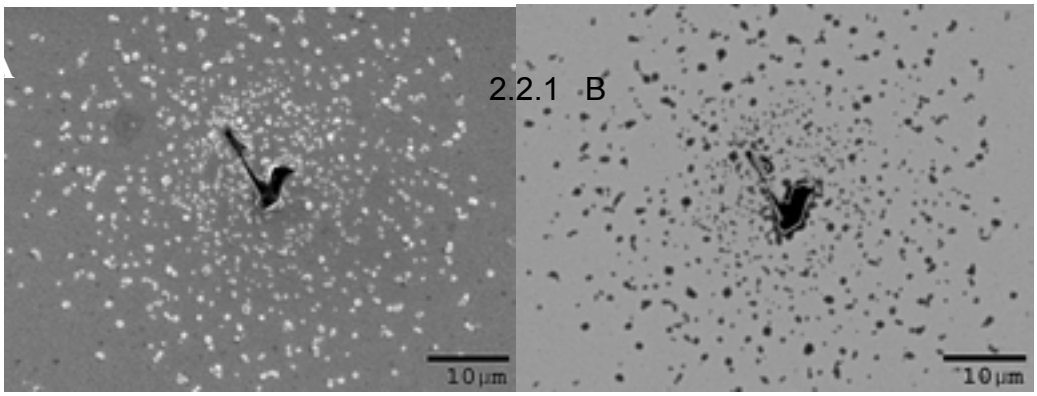

Photomicrograph 2 – (a) secondary and (b) backscattered electron images of TC defect voids caused by large NaCl crystal formation. The large crystal dissolved during washing and partially precipitated as small NaCl crystals (light in (a), dark in (b)) near the defect.

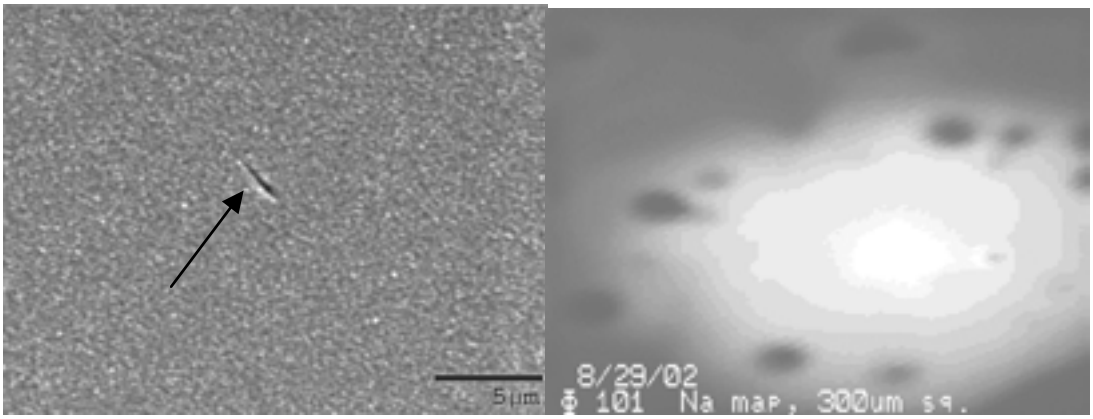

a b

Photomicrograph 3 – The source of a ~400µm diameter non-coloring area was traced back to a small crack in the TC layer ~3µm long. (a) Secondary electron image showing the defect center showing a small crack and (b) a sodium secondary ion map of the non-coloring area (note scale difference between (a) and (b)—full frame is *ca.* 300µm wide). The white region (highest [Na]) is at the defect center. The radius of the non-coloring area corresponds to the Na diffusion distance from the central crack.

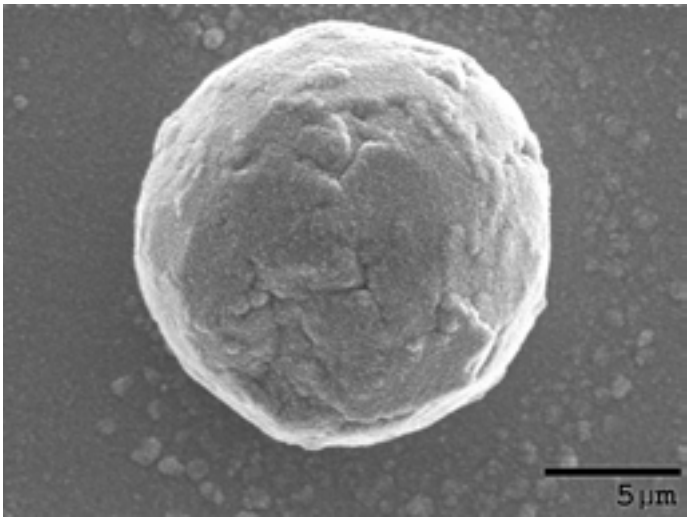

Photomicrograph 4 – Tin speck on TC surface formed during the TC deposition process. The spheroid is approximately an order of magnitude larger than the electrochromic film thickness and interrupts the thin film stack, creating a localized short.

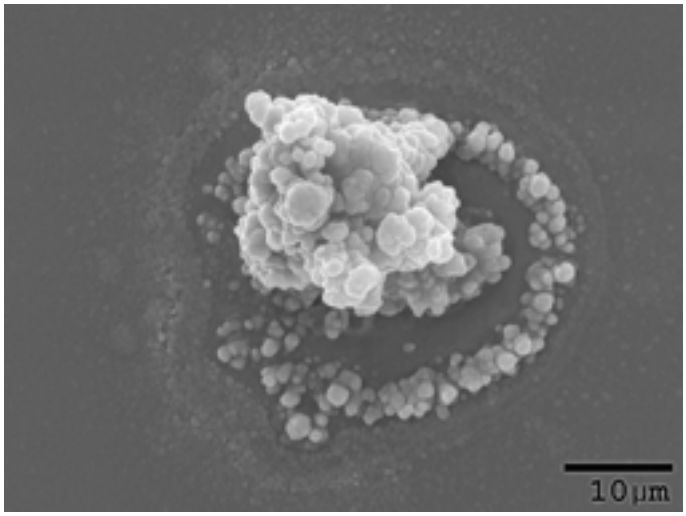

Photomicrograph 5 – Device short related to contamination generated in bus bar manufacture.

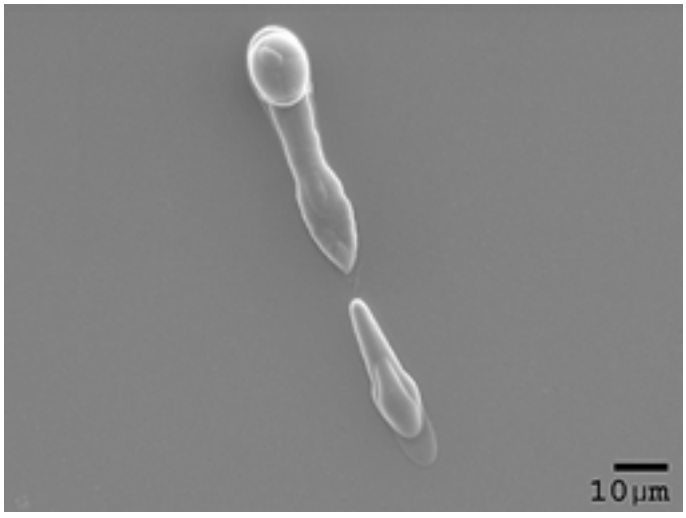

Photomicrograph 6 – Device short related to ejecta from arcing from a stainless steel substrate carrier.

II.2 CE MODIFICATIONS

The CE in electrochromic devices is a critical layer. It is used to store the charge, which is used to color the electrochromic layer (in our case the WO_3) when the device is in the clear state. It must therefore have several properties: (i) It must allow charge to intercalate easily; (ii) it must be stable and durable to repeated cycling; and (iii) to maximize the clear state transmission, it must display little or no absorption in the fully intercalated state. SageGlass® windows use a proprietary mixed oxide composition that has all these properties. The as-deposited CE film is highly absorbing, but during device processing, as the charge is introduced into the system, this absorption is bleached out.

The counter electrode (CE) used in the SAGE device has been shown to be very stable to repeated charge insertion/extraction cycling, but may possibly display a small amount of residual absorption when the device is fully bleached. This leads to a slight coloration in the bleached state. This absorption, although acceptable for some applications, is unacceptable for vertical windows, particularly in the residential market sector. The challenge is to remove this absorption without sacrificing the wide dynamic range and good switching kinetics of the device.

The CE we use is a thin film of a confidential metal oxide mixture, which we will refer to as $A_aB_b...N_nO_x$, where *a* is the percentage of metal A by weight, *b* is the percentage of metal B, etc., and *x* is the mole fraction of oxygen. We are currently using a CE with a particular composition for our pilot line studies, and this is referred to as CE-I. Further CE compositions will be distinguished as CE-II, etc.

The work reported here will concentrate on experiments carried out with one particular target with an increased concentration of metal A, labeled CE-II.

II.2.1 Variations caused by different CE compositions

Thin films from target CE-II were deposited in the lab coater to determine sputter deposition conditions that would yield thin films with properties suitable for our application. It was found that for similar deposition parameters, a number of properties in the as-deposited films were different from those obtained from CE-I.

The sputter rate was faster for CE-II when compared to CE-I resulting in film thicknesses approximately 30% greater than for the “normal” CE (CE-I). Naturally, this will only be significant if the thickness requirements for the CE remain the same for the different composition, but an increase in deposition rate is obviously beneficial when we move into a production setting, as it will potentially reduce capital outlay and/or cycle time.

The film deposition described above yields a transmission (as-deposited) for the CE-II film which is ~25% greater than for CE-I, indicative of the changed composition.

Work carried out to understand the optical properties that can be obtained from the two different CE compositions has focused on depositing CE/Li/ITO stacks on witness slides, and studying the optical properties of these, without the complications of the underlying TC/WO_3/IC layers. In addition, some CE films have been deposited onto glass coated with the TC to study the electrochemistry to ensure that this is still adequate for our purpose.

Optical measurements of CE-I vs. CE-II. Samples of CE-I/Li/ITO were deposited onto clear glass slides and the optical properties determined. Some samples were heated, and the optical properties re-measured. Some typical data are given in Table II.5 in the Appendix. We note that the transmission and color coordinates for this partial stack are reasonably close to those obtained for the whole device, so it is reasonable to assume that any improvements in optical properties which we can make on this partial stack will be transferred over to the whole device. We will

focus on b* as the parameter which we need to control. In general we find a range of b* values for these stacks, and this is reflected in the values we measure in finished devices.

Our aim is to increase the visible light transmission, (T(%)) and reduce the value of b* to somewhere close to zero without compromising the charge capacity or electrochemistry. Samples of CE/Li/ITO were deposited in an identical way, but this time using the CE-II target. Some values for the same measured quantities are given in the Table II.6 in the Appendix. It is clear that b* is lower for the majority of these films than the values we see for equivalent CE-I stacks. It is therefore assumed that using the new CE composition will lead to a reduction in b* for our devices.

Electrochemical Measurements CE-I vs. CE-II. The electrochemistry of CE-II films looks very well behaved and reversible. A cyclic voltammogram (CV) of lithiated CE-II is shown in Figure I.3. (For details on measurement and interpretation of CVs, the reader is referred to A.J.Bard and L.R.Faulkner 'Electrochemical Methods', Pub: Wiley (1980), Chapter 6). In this measurement the voltage between the thin film of interest and a reference electrode (in this case lithium metal) immersed in the electrolyte is measured, and recorded. This is the open circuit voltage, V_{oc}. The voltage then is swept at a controlled rate (in this case 20mV/s) from V_{oc} to some predefined anodic and cathodic limits and the current recorded. A flow of current represents an electrochemical reaction between the electrode and the species in the electrolyte, in this case lithium insertion and extraction. The transmission of the film using a diode laser and photodetector is measured at the same time as the CV so that the optical changes can be related to the electrochemistry.

Features in a CV can be interpreted in terms of the electrochemical processes which are occurring and can lead to a better understanding of the electrochemistry of the CE films, and hence the overall behavior of the device.

In the example shown in Figure II.3, where we illustrate a typical CV, there is a clear separation between different lithium insertion reactions. Beginning at approximately 3.0V vs Li, the voltage is first swept to higher potential, i.e. 4.5V vs Li, and a (negative) current flows out of the electrode. This is indicative of electrons flowing out of the electrode into the external circuit, and positively charged ions being ejected into the electrolyte. The voltage is now swept back to a less positive value, and charge is re-inserted into the CE film. As the voltage is swept further, the current reaches a limiting value, (dependent upon the sweep rate and the charge capacity of the film), and then reduces back towards zero. A second charge insertion peak can be seen at voltages below 2V vs Li. As the sweep direction is once again reversed, this cycle is repeated.

Given the behavior we see here, we can be confident that films deposited from the CE-II composition target will show good electrochemical behavior when used in an EC device.

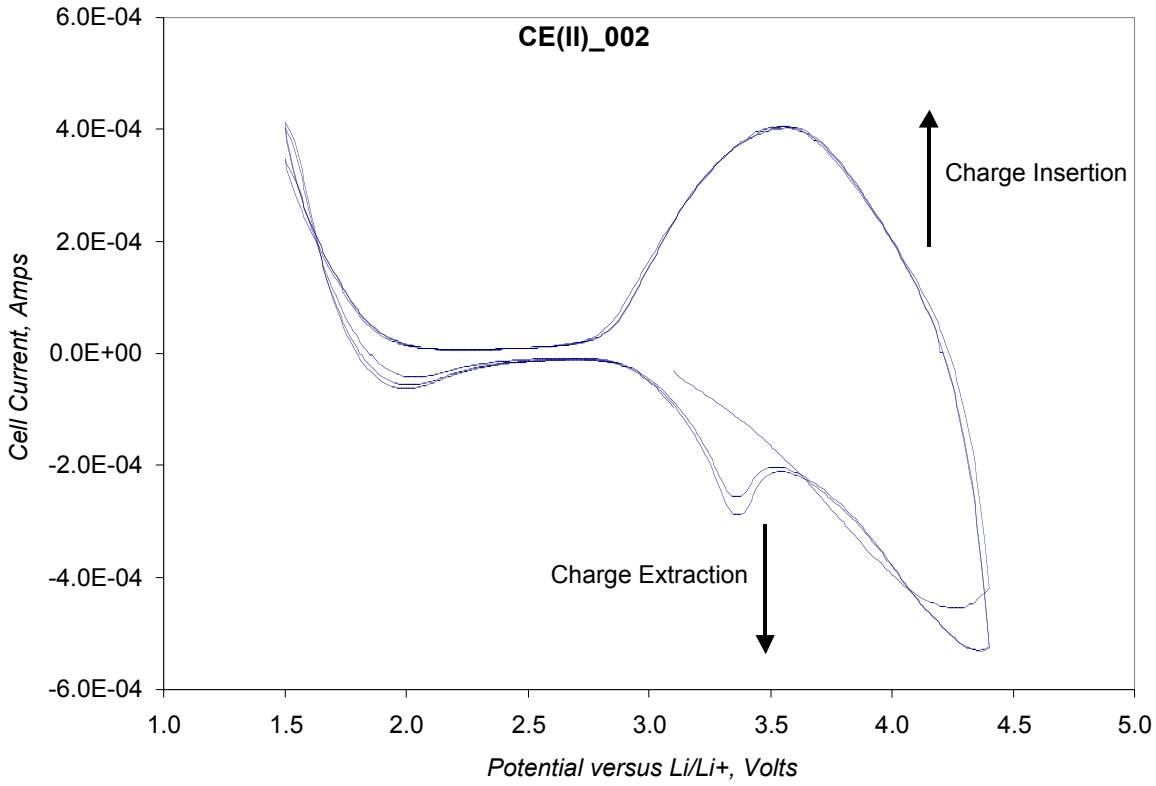

Figure II.3 – Electrochemical measurements of a CV of a sample of CE-II in a lithium containing electrolyte. Sweep rate was 20mV/s and the sample area was 4cm^2. The open circuit potential was approximately 3.1V vs. Li/Li$^+$.

II.2.2 Impact of gaseous dopants on structure and interface characteristics of CE

The absorption of the CE film is an important indication of the state of oxidation of this layer – higher absorption indicates a more oxidized film. It is important to maintain consistency of the oxidation state of this film to maintain consistency of the performance of the final product, as this is likely to affect the optical properties and the electrochemical behavior of the layer.

Single layers deposited on clear glass on the pilot line coater have shown variation in the thickness and absorptivity which appear to be related to the background contamination (base pressure) in the sputtering machine. This is shown in Figure II.4 where the value of *k* at 500nm[7] is taken as a measure of the absorption for these films. These films were all deposited under nominally identical conditions during a relatively short period of time. There is a clear spread in these data, both for the absorption and the thickness, hence this study to determine which contaminant gas or gases are responsible.

[7] *k* is determined by measuring both the reflection and transmission of the film, and then fitting an optical model to these data. The variables in the fit are the optical constant (*n* and *k*) and the thickness.

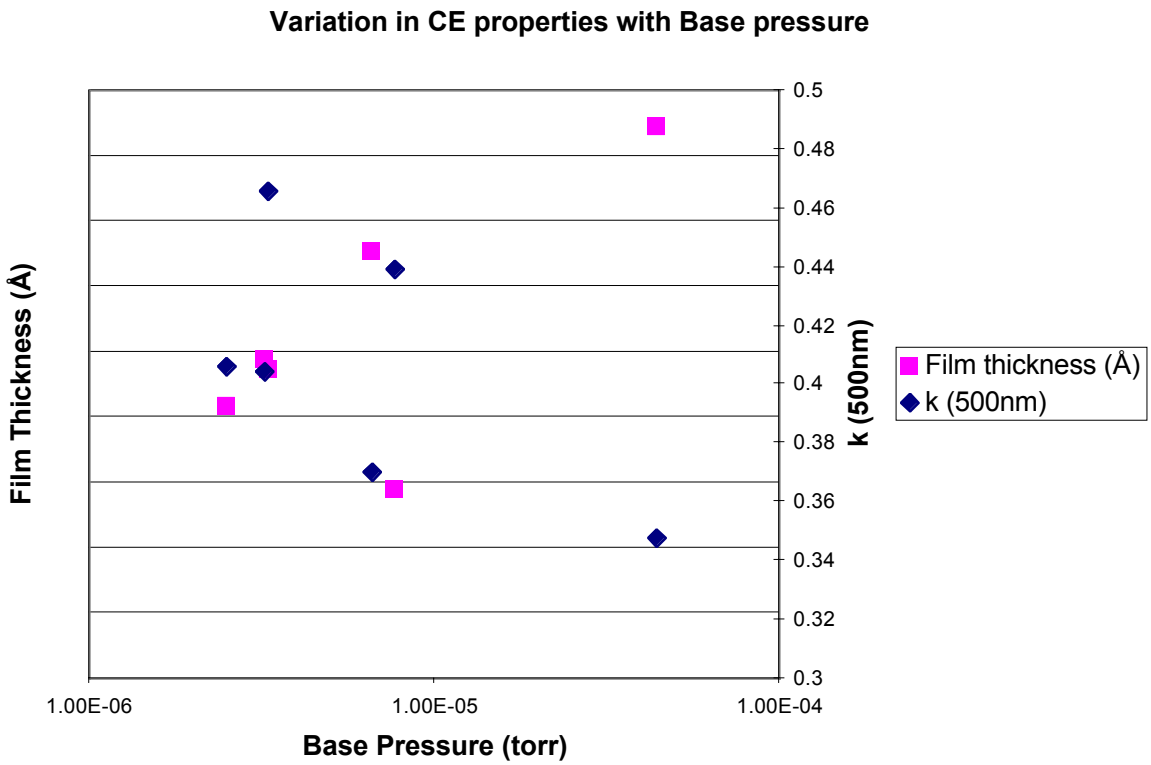

Figure II.4 – Variation in CE film properties shown as a function of base pressure for films deposited in the pilot line sputtering machine. All films deposited under the same conditions.

To investigate this, a study in the lab was undertaken. Single layers of CE were deposited onto 3" x 1" glass slides under various well-controlled conditions. The transmission and reflection spectra of these layers were then recorded, and from these data, the thickness and optical constants determined. Different gas compositions were used to determine the effects of small amounts of background impurities on the properties of the CE films.

The nitrogen, CO_2 and argon additions to the oxygen sputtering environment were simply obtained by using a separate gas bottle and flow controller. The water was added by bubbling oxygen through water—held at or close to 0°C—and then diluting this with dry oxygen to obtain a variety of different water levels. The bubbler was fitted with a diffuser to ensure the highest contact of gas with water.

Each film was deposited after allowing the chamber to pump down for at least 30 minutes; generally this meant that the chamber pressure was less than 3×10^{-6} torr, and the target was pre-sputtered for 30 minutes prior to film deposition.

The nominal conditions for the CE deposition are proprietary. Several films were deposited under standard conditions from time to time throughout the study as a check. The repeatability of the results from this series shows that there is no long-term drift of the process.

(a) Effect of Argon

Argon was added to the standard sputtering gas and some oxygen was removed to maintain approximately the same pressure. The deposition conditions were therefore slightly modified from the standard conditions. The number of passes was reduced to maintain the thickness close to a target thickness when it became apparent that adding Ar increased the deposition rate.

The results for a number of different depositions are shown below in Figure II.5, giving some idea of the repeatability of this measurement. Clearly, there is little or no effect on the absorption of these films, but the deposition rate is considerably enhanced by addition of argon. Note that several of the films deposited with Ar were made with double the number of passes, but there is no significant difference seen—except the obvious thickness difference—the thickness deposited per pass remains the same. Note the spread of data for the absorption is very similar both with and without argon, indicating no effect of argon on the film properties at this level.

We can conclude that a useful increase (a factor of two) in deposition rate was achieved by the addition of small amounts of argon, with no apparent change in the optical properties of the films. It is likely that further increases in deposition rate are possible by further argon addition. This will be useful in two ways: (i) The requirements for cathodes/deposition zone in the production coater will be reduced; and (ii) because the film is deposited faster, there will be less deleterious impact of the effective concentration of background residuals incident on the growing film.

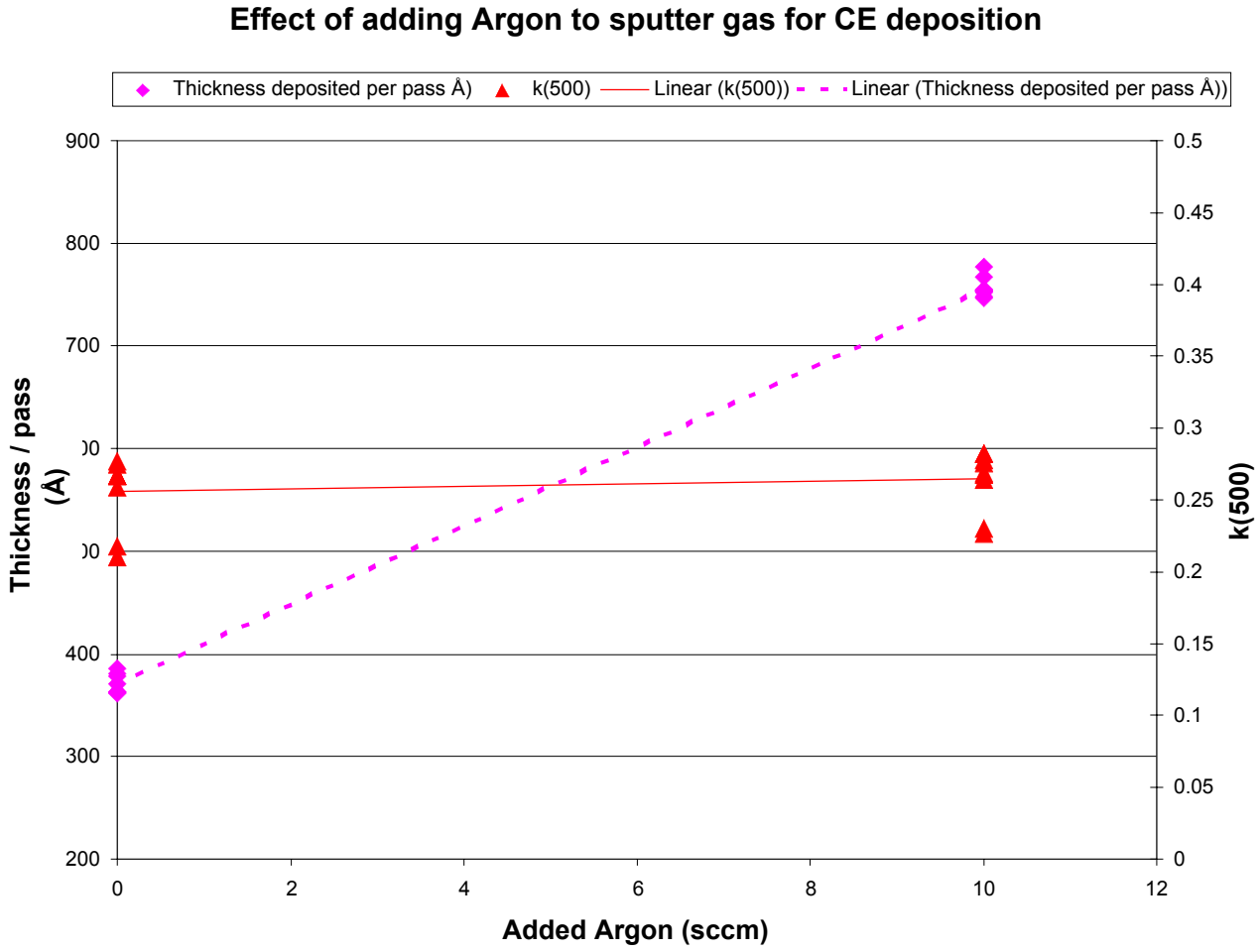

Figure II.5 – Effect of argon addition on the deposition rate and optical absorption of CE films deposited in the lab coater. Conditions for the films deposited with argon added are given in the text.

(b) Effect of water addition

Water was added as described above, by bubbling oxygen through ice water in a bubbler held in a water bath at zero deg C. Using this arrangement, fully saturated oxygen containing approximately 6000ppm by volume (or 3640ppm by wt) were produced.

The results are shown in Figure II.6, where the data are plotted as a function of wet oxygen flow – 60sccm represents 100% wet oxygen flow, and is therefore as saturated as possible. Very little effect is seen on either the thickness or the absorption, although there may be a slight decrease in absorption (results are plotted as the reciprocal of *k*(500nm)) with increase in the level of water. It is assumed, however, that the residual water levels in the pilot line will not reach the extremely high levels seen here.

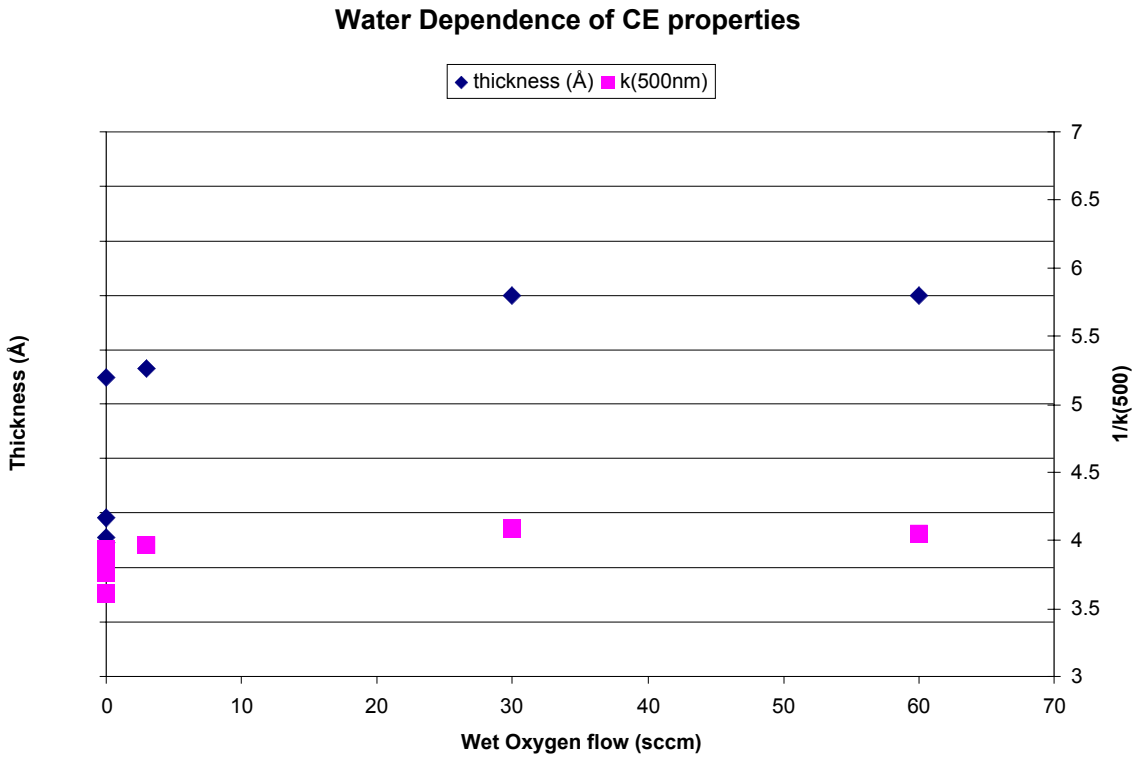

Figure II.6 – Effect of water addition on the deposition rate and optical absorption of CE films deposited in the lab coater. Conditions for the films deposited with water added are given in the text. A wet oxygen flow of 60 sccm corresponds to approximately 6000ppm.

(c) Effect of Nitrogen

Nitrogen was added to the sputter gas and the results of the thickness measurements are given in Figure II.7. Several other data points are shown for samples that were deposited (a) at slightly higher temperatures (around 150°C) and (b) some with an addition of CO_2. All of the measurements show little or no dependence of the thickness on any of these parameters. We see very good consistency of thickness reproducibility.

Figure II.8 shows the measured absorption for the same films as a function of nitrogen addition, and also for the films with added CO_2. We can see an increase in the value of *1/k* (the reciprocal of absorption shows the same trend as the transmission), hence an increase in the level of nitrogen produces an increase in the transmission of the film. (We see a similar trend for the CO_2, but this is less of an effect than for the nitrogen.)

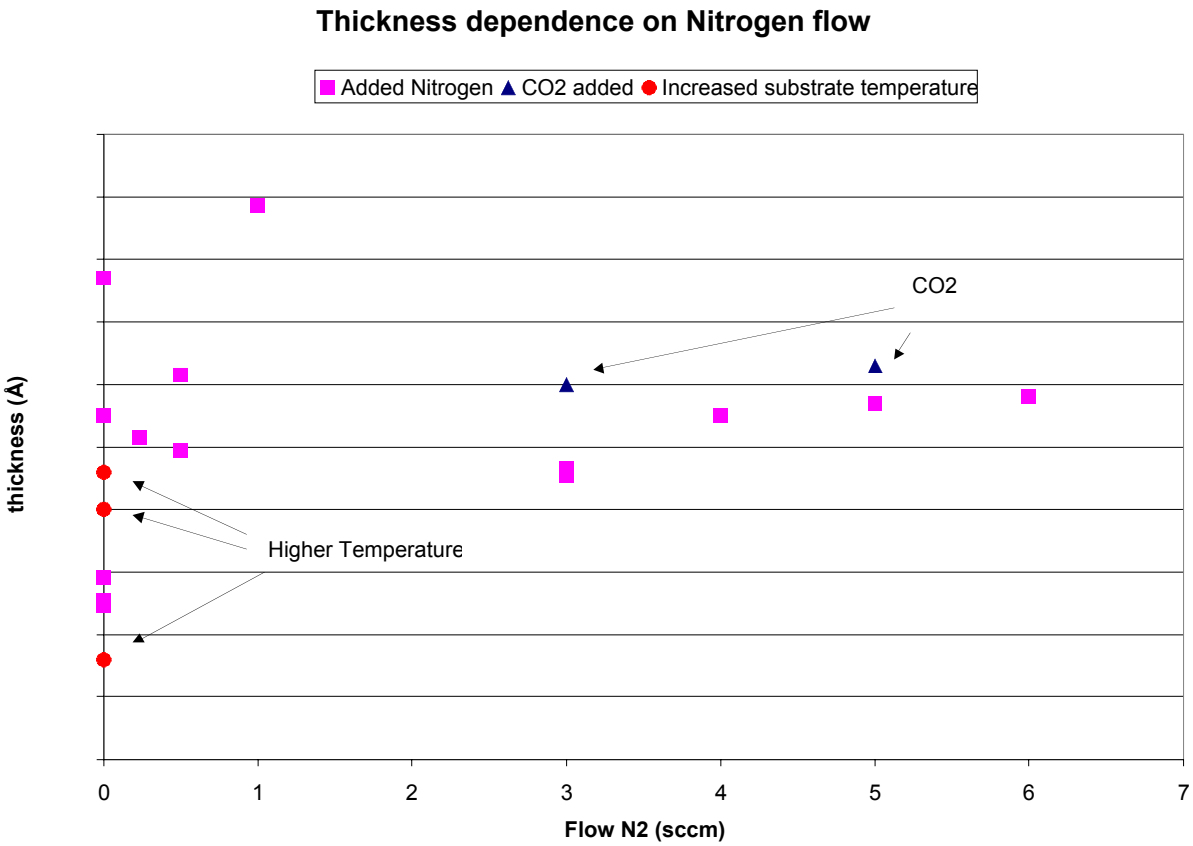

Figure II.7 – The thickness dependence of films grown with different levels of nitrogen contamination. In addition, several films deposited at elevated temperature (red circles) and two films deposited with CO_2 addition (blue triangles) are also shown. Note there is no dependence of thickness on either N_2, CO_2 or heating.

Increases in *1/k* from around 4 to around 6 represent a transmission change from ~33% to ~48%, which is a significant difference.

It is clear that a small air leak into the coater could have a significant effect on the properties of the CE layer. This is most likely to be a result of the nitrogen rather than the CO_2 because of the higher percentage of nitrogen in the air compared with CO_2.

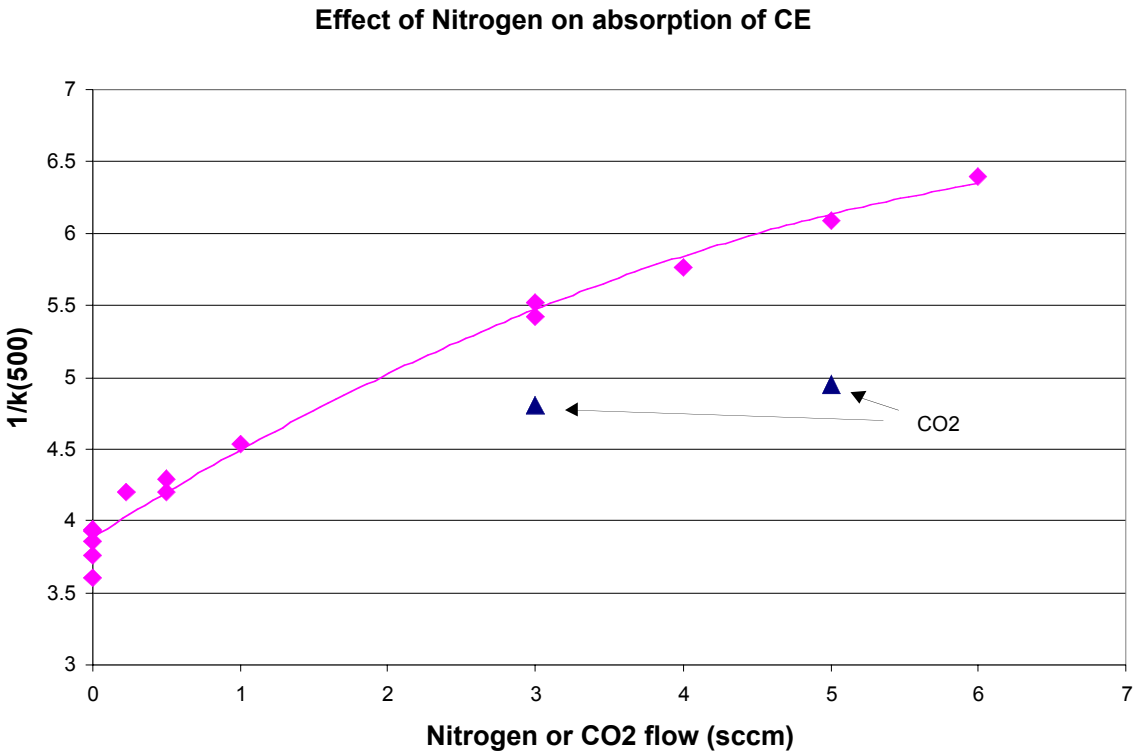

Figure II.8 – Effect of adding nitrogen to the sputtering gas on the measured absorption for a number of thin films. The values for CO_2 are also shown for comparison.

(d) Effect of CO_2

As seen above, the effect of CO_2 seems to decrease the absorption, but has little effect on the thickness. The magnitude of the absorption change seems to be about a factor of 2 less than that from nitrogen.

The optical properties of the CE have been found to be sensitive to nitrogen and CO_2 and insensitive to water and low level heating. This can be summarized as follows:

Contaminant	*Absorption*	*Thickness*
Argon	No effect	Increases
Nitrogen	Decreases	No effect
Water	No effect	No effect
CO_2	Decreases	No effect
Temperature	No effect	No effect

Table II.7 Effects of contaminants on CE properties.

So far, nothing except Ar has been found which would give rise to the increase in thickness with increasing base pressure seen from the data given in Figure II.4, but residual levels of nitrogen from the air can easily explain the differences we see in optical properties.

II.2.3 Modifications to the CE sputtering process

Variations in the optical properties of the CE continue to be an issue for us. Figure II.9 shows the measured transmission for witness pieces deposited onto glass slides in the pilot line coater. The six witness pieces from each run are spaced evenly across the width of the cathode. Each "string" of joined points represents measurements of transmission taken from one run, and in most cases there are six points. The point on the left of the string represents the console side sample, and that on the right represents the pump side. Any variation in a string indicates a "side-to-side" variation. All of the films discussed here are deposited under nominally identical conditions, where the power, pressure, gas composition, line-speed and number of passes[8] are all held constant. The pressure is held constant by continually adjusting the gas flow into the slot using a closed loop feedback. The data here represent witness piece runs carried out since March 2002.

We can see that there is a clear variation in the transmission as a function of time. Furthermore, during the early runs, we can see a definite side-to-side variation in the optical properties of the CE, i.e. in a direction parallel to the target. This is seen as a hump in each data string prior to the point at which a new target was installed. Following the installation of the new target, the shape of each string changed to be more indicative of a gradient from one side to the other.

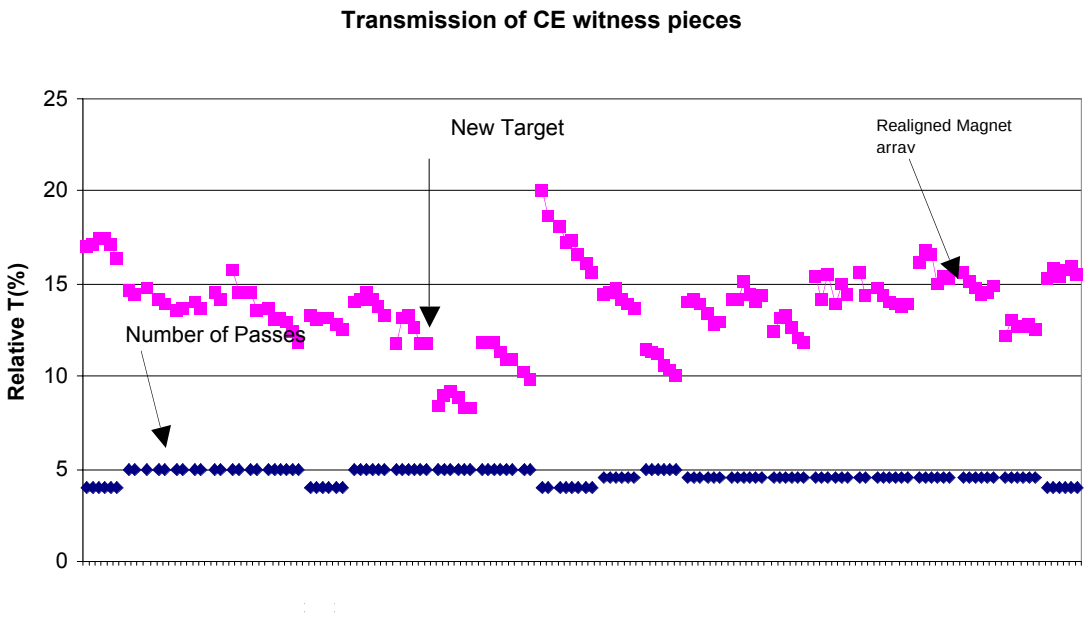

Figure II.9 – The variation of transmission (relative) as a function of run number showing a significant process variation. The number of passes is also indicated, showing that there is some correlation, but this is insufficient to explain the variation seen here. Each "string" of joined points represents one run, in most cases there are six points.

[8] In some instances the number of passes are altered but this is noted and shown in Figure II.9.

Consider first the variation within a run, i.e. the side-to-side variation. We have contemplated several possible causes for the variation within a run. Prior to installing the new target, there was a question as to whether the tiles of the target were bonded sufficiently to the backing plate. Indeed any voids in the bonding would likely lead to a different deposition rate from that particular tile. This was seen to be the case when the target was removed, and hence can now be eliminated as a problem.

The side-to-side variation seen in the strings of six points is clearly visible even after we changed the target, but does not seem to be consistent run to run. As this is an absorbing film, both the thickness and the absorption will determine the transmission. We have been deriving the optical constants and thickness from transmission and reflection measurements, and find that while there is some variation in both parameters, we are most concerned with the variation in the absorption, as this is indicative of a variation in the physical properties of the film itself. We have found that it is possible to obtain such a variation in at least two ways: (i) the oxidation state of the film may increase, leading to a more highly absorbing film; or (ii), the ratio of the constituent materials may vary. We have been investigating both possibilities, and in collaboration with the target manufacturer, have made a thorough investigation of the target stoichiometry and density.

We have recently made some adjustments to the magnetic array in the CE cathode. This seems to have resulted in a fairly marked improvement in thickness uniformity across the target, from something on the order of 5% before the change, down to a variation of less than 2%. This is shown in Figure II.9.

We investigated the composition of deposited CE films, as there was some question as to whether the molar ratio of the constituent metals was varying across the target, resulting in the non-uniformity. The standard sample preparation technique for atomic absorption analysis had to be modified since one of the sample constituents was not completely dissolved in the analyte solution. We developed a new technique to ensure that complete dissolution of the components in the films occurred, and subsequent results from atomic absorption analysis of witness piece samples showed that there was no appreciable variation of composition across the target.

The original run-to-run non-repeatability for the CE deposition has proven to be more troublesome to track down. We have seen that the level of background impurities has a significant effect on the properties of the deposited film, and this can be seen in Figure II.10, where both the base pressure prior to deposition is recorded, along with the measured device transmission after CE deposition. Clearly, these measurements have the same trend with time, but this is an insufficient condition to assert that this is causal. However, the similarity is compelling, and so we will attempt to determine the origin of the base pressure variation in order to remove this variable from our process.

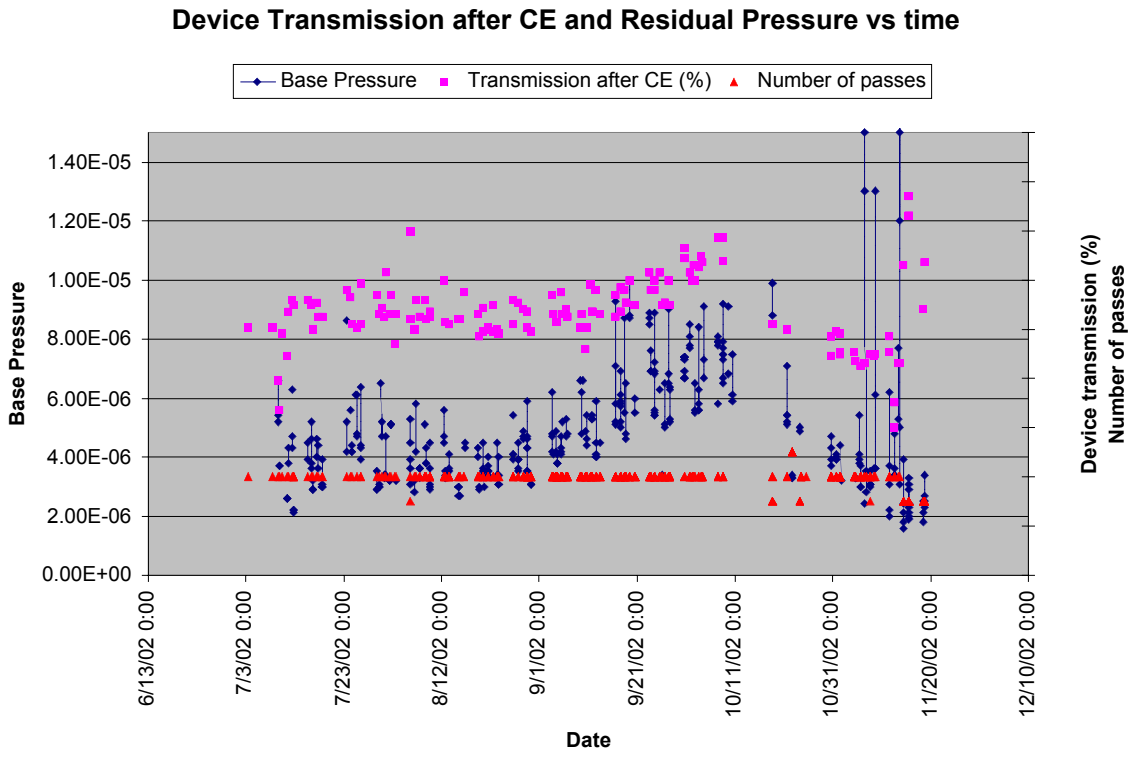

Figure II.10 - The base pressure of the coater prior to CE deposition as a function of time, plotted alongside the measured device transmission after CE deposition. The number of passes across the target is also shown as this will alter the thickness of the CE film, and hence the measured transmission.

In conclusion, we have made significant progress in understanding and controlling the process parameters that affect the CE deposition. We have tightened our process limits as a direct result of the work on background contamination of the CE. In addition, we have made significant changes to the cathode to improve the uniformity across the target for around 5% at the beginning of the project, to below 2% currently.

II.2.4 Alternative CE materials (begun in 2002 and will continue in next phase)

In addition to varying the constituent concentrations of the present CE, we will pursue some alternative materials with the goals of achieving more neutral coloration and greater dynamic range. This work will be carried out in Budget Period 2.

II.3 SECOND GENERATION ION CONDUCTOR

The IC layer in the SageGlass® EC device uses a patented proprietary technology which gives excellent optical, ionic and electronic properties. However, by altering the structure and composition of the IC we can fine-tune the refractive index and conductivity, thereby maximizing the transmission range, uniformity and switching rate of our EC device. Details of the IC materials and characterization are proprietary and included in the Appendix.

III. SOLID STATE MODEL OF EC DEVICE

III.1 BAND THEORY MODEL OF RELATIONSHIP BETWEEN OXIDATION STATES OF WO_3 AND COUNTER ELECTRODE AND CURRENT VOLTAGE CHARACTERISTIC OF DEVICE. IMPACT ON LEAKAGE CURRENT AND ABILITY TO SWITCH LARGE DEVICES

Understanding the electronic behavior of SageGlass® devices is important because it will allow us to determine the parameters that dictate the electronic leakage currents through the stack. In good devices, the leakage current appears to behave as if the device were a diode. An example of this is shown in Figure III.1. An understanding of the relevant parameters could conceivably allow us to extend the depth to which we can color the device, thus increasing the dynamic range.

In this work, we have tried to isolate the origin of this diode-like behavior by constructing a range of samples with different structures in an effort to isolate the interface, or interfaces which lead to the electronic behavior we observe. Each different structure is considered in the following sections.

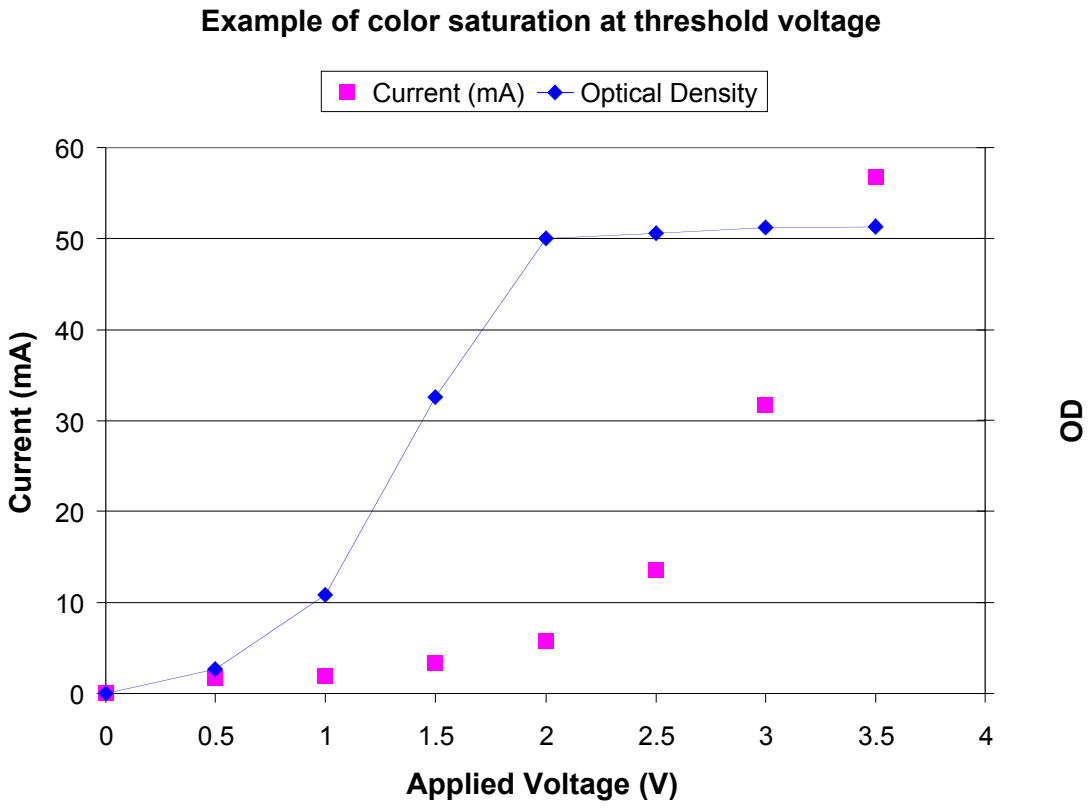

Figure III.1 – An example of electronic breakdown leading to saturation of the optical density of an EC device.

Electronic behavior of samples with no CE layer

Samples were deposited with no CE layer in an attempt to investigate the origin of the diode in the device. Static electrical measurements for two configurations are reported in Figure III.2: TC/WO_3/IC/ITO and TC/WO_3/ITO. We see that the IC clearly results in a decrease in the current through the stack, but does not give the asymmetrical diode-like characteristic that we see in Figure III.1. In fact, the sample with no IC appears to be almost ohmic in behavior, so we can probably rule out the TC/WO_3 interface as a cause for diode-like behavior.

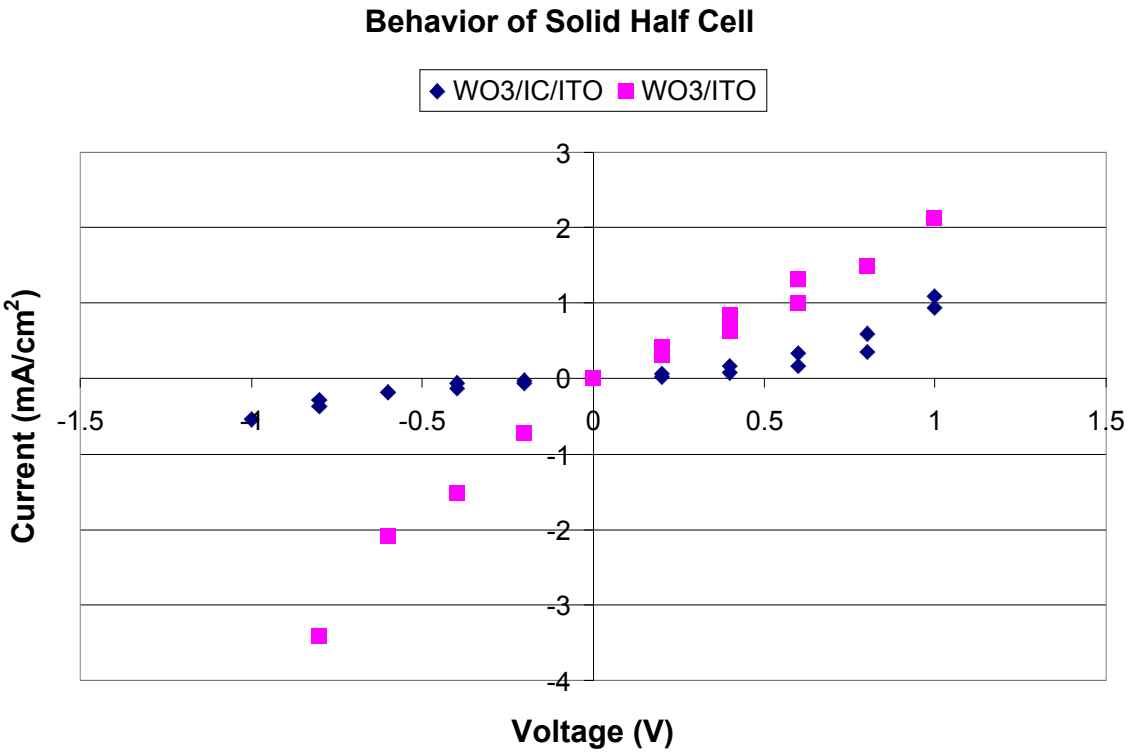

Figure III.2 – Static electrical characteristics of two partial stacks: TC/WO_3/IC/ITO and TC/WO_3/ITO.

Electronic behavior of samples with no WO_3

A set of samples with no WO_3 was fabricated, and the electrical behavior was measured and is reported in Figure III.3. It is clear that the diode-like characteristic is not evident here either. There is evidence of hysteresis, and this may indicate charge trapping somewhere in the stack, although this has yet to be confirmed.

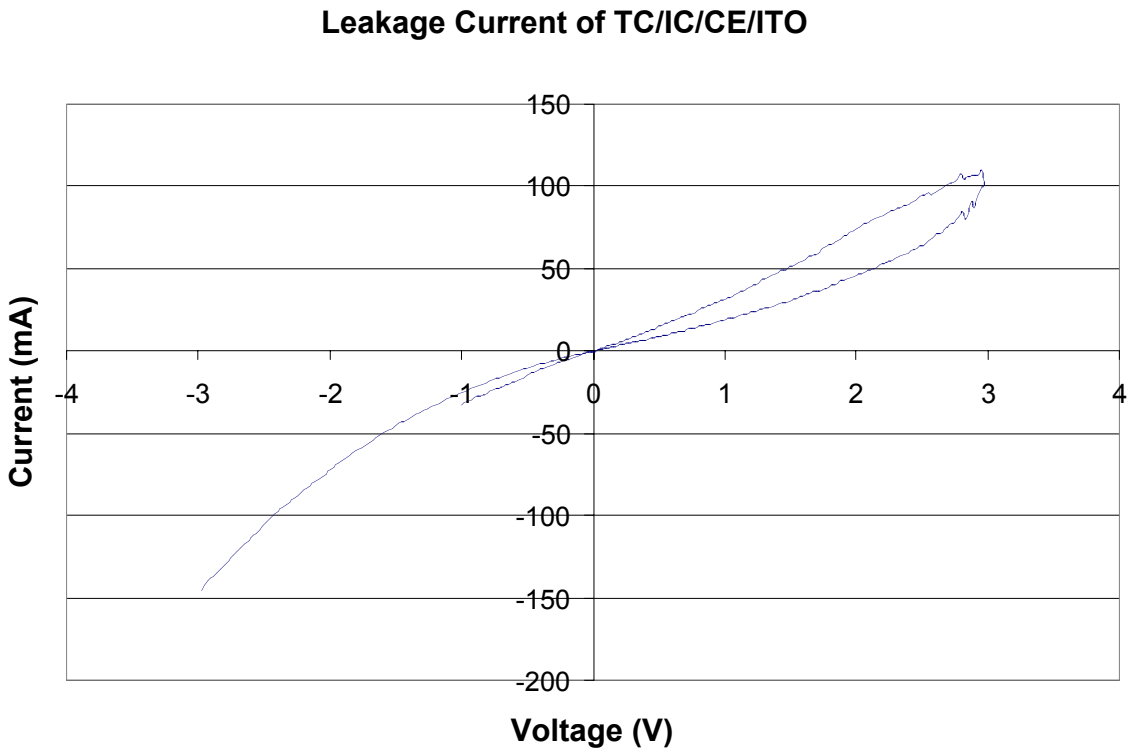

Figure III.3 – Electrical characteristics of device made with no WO_3.

Electronic behavior of WO_3-IC-WO_3 samples

To determine whether the diode can be due to the WO_3-IC interface, samples of WO_3-IC-WO_3 were deposited onto conductive substrates, and a top contact of ITO deposited to allow electrical measurements to be made. Typical data are shown in Figure III.4, where once again we see no evidence of rectifying behavior. It is therefore reasonable to eliminate this interface as the cause of the electrical behavior seen in EC devices.

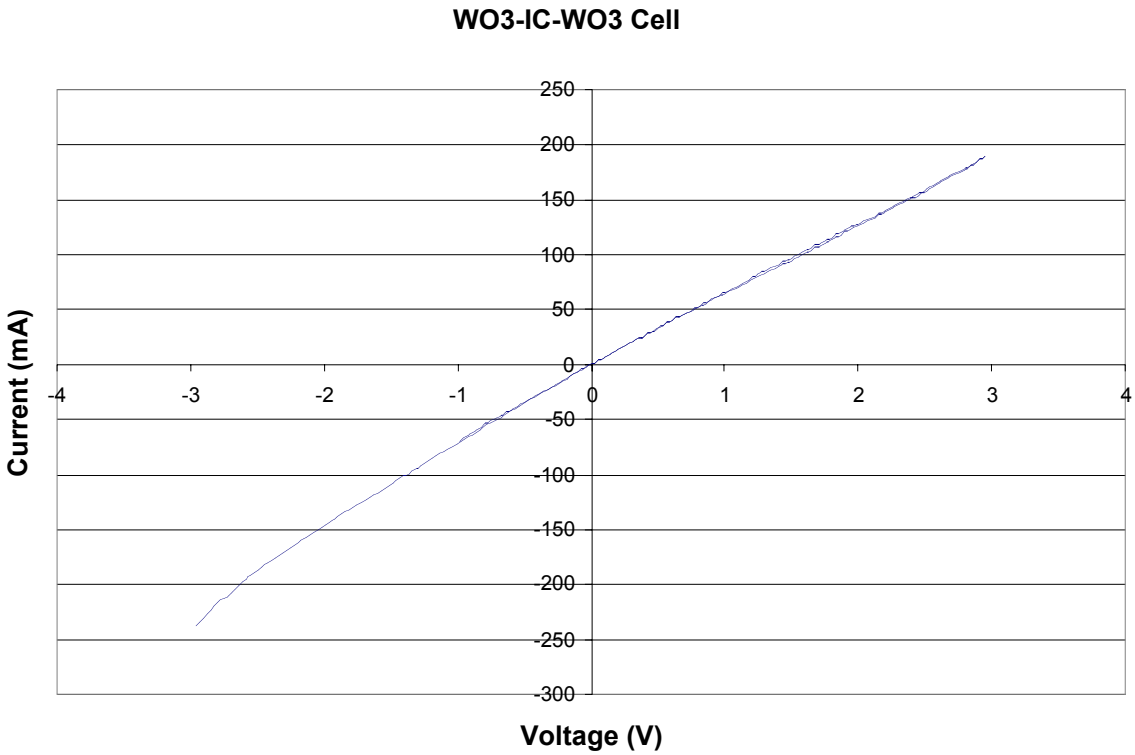

Figure III.4 – Electrical measurements of a sample of WO_3-IC-WO_3 showing no rectification.

Electronic behavior of CE-IC-CE samples

Samples of CE-IC-CE were fabricated in a similar way to that described in the previous section, and the electrical measurements for a typical sample are shown in Figure III.5. Once again, we see no evidence of rectification. Note that there is no lithium inserted into this sample, so we only see the effect of the CE-IC junction.

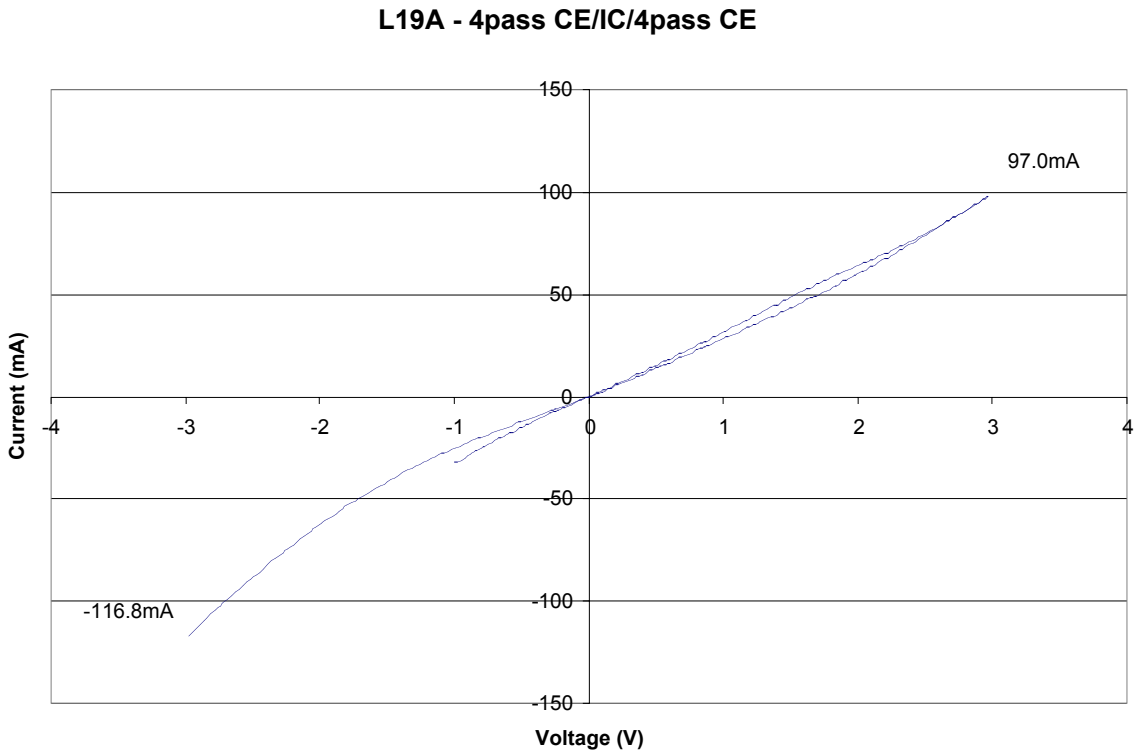

Figure III.5 – Electrical measurements of a sample of CE-IC-CE showing no rectification.

Electronic behavior of WO_3-CE samples

Once again, samples of WO_3/CE were deposited onto a conductive substrate and a top contact of ITO deposited to allow electrical measurements to be made. Rectifying behavior was seen in all the samples made, even where the CE thickness was reduced to 300Å. An example of this is shown in Figure III.6.

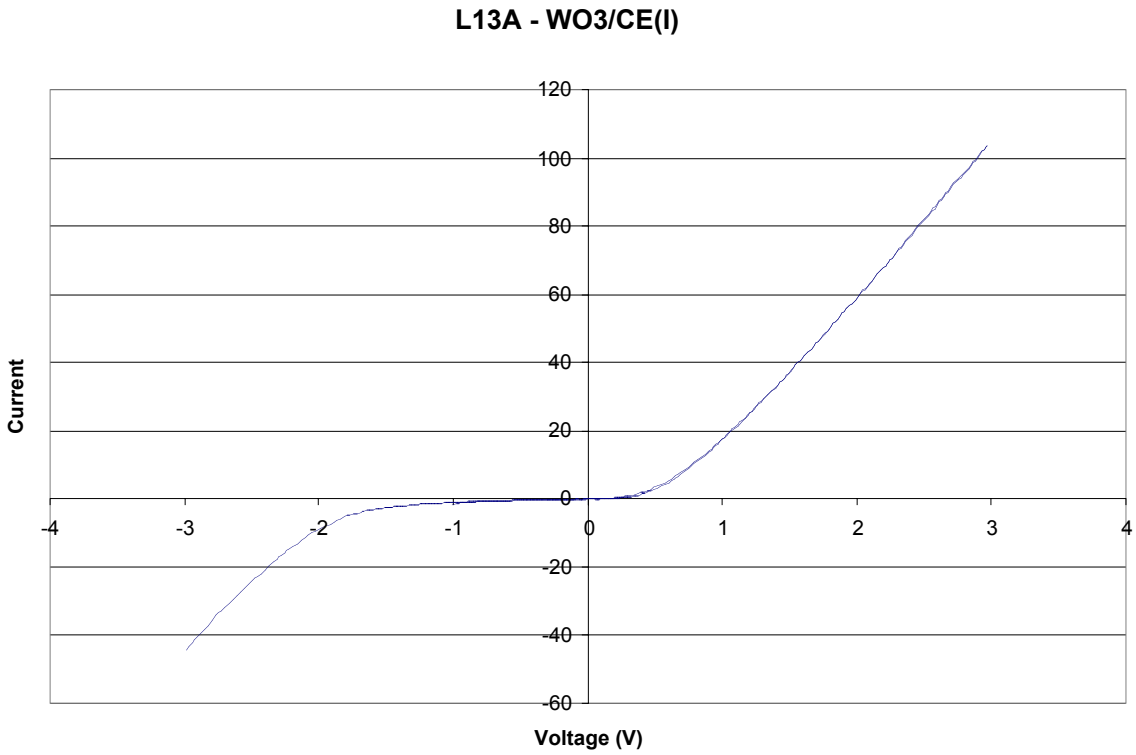

Figure III.6 – Example of electronic behavior of WO_3/CE junction, showing clear evidence of rectification in both forward and reverse direction.

In all cases, the turn on voltages were about 0.5V for the forward direction, and 2.0V for the reverse direction. Variations in the thicknesses of the layers did not make significant differences to these voltages as can be seen from Figure III.7. In addition, the slopes of the linear portions of the I-V characteristic subsequent to turn-on correlate extremely well to the resistance of the transparent conductors.

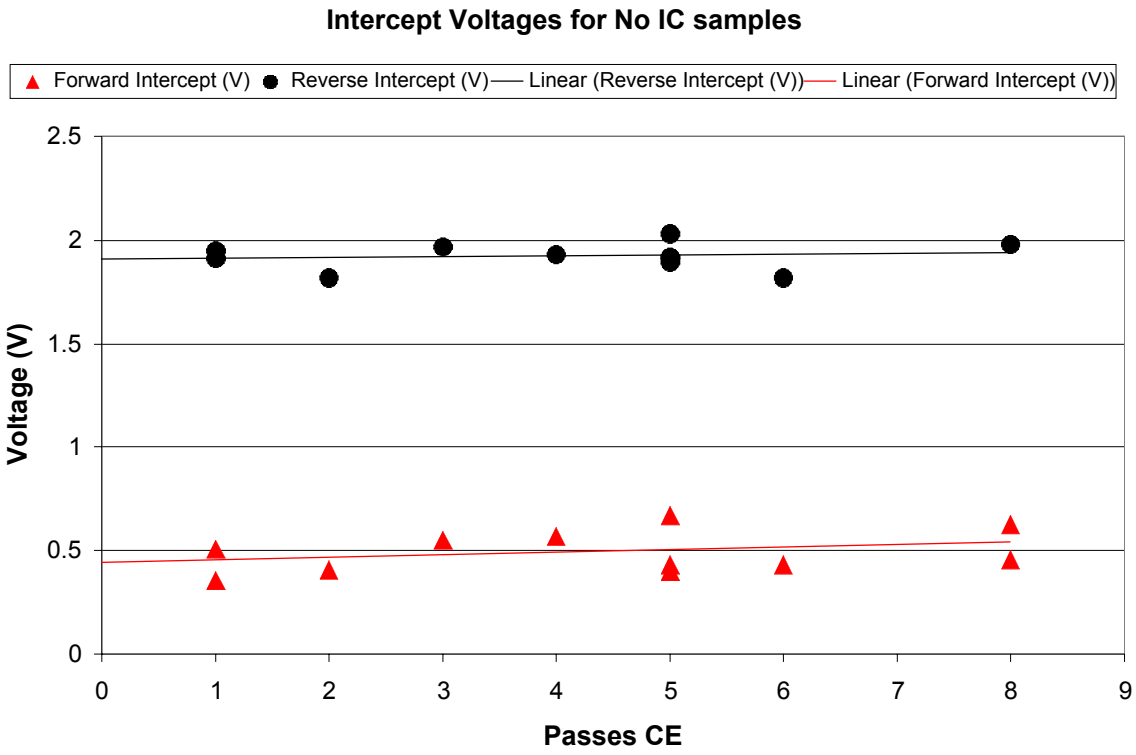

Figure III.7 – Intercept voltages plotted against number of passes of CE (equivalent to CE thickness) showing little or no variation.

From this short study, it appears as though the origin of the diode-like behavior is the junction between the CE and the WO_3. Further proprietary modification of the CE/WO3 junction yielded the very significant result shown in Figure III.8 in the Appendix. The forward turn-on voltage has been increased from 0.5V to ~1.7V permitting deeper coloration and assuring the capability to switch larger devices (i.e. those with dimensions greater than 20").

Summary of electronic behavior of samples

We have seen that the determining factor for the electronic response of SageGlass® devices is the junction between the WO_3 and the CE. The measured turn-on voltages do not depend on the thickness of these layers. We have found that the IC will stabilize this characteristic during subsequent processes. The exact mechanism for this is unclear. Generally, we are not able to make devices without IC that switch well. Part of the reason may be related to the modification of the electronic barrier between the WO_3 and the CE upon subsequent processing. Recent attempts to fabricate such devices generally end with a "leaky" system that does not switch well. An example is shown in Figure III.9.

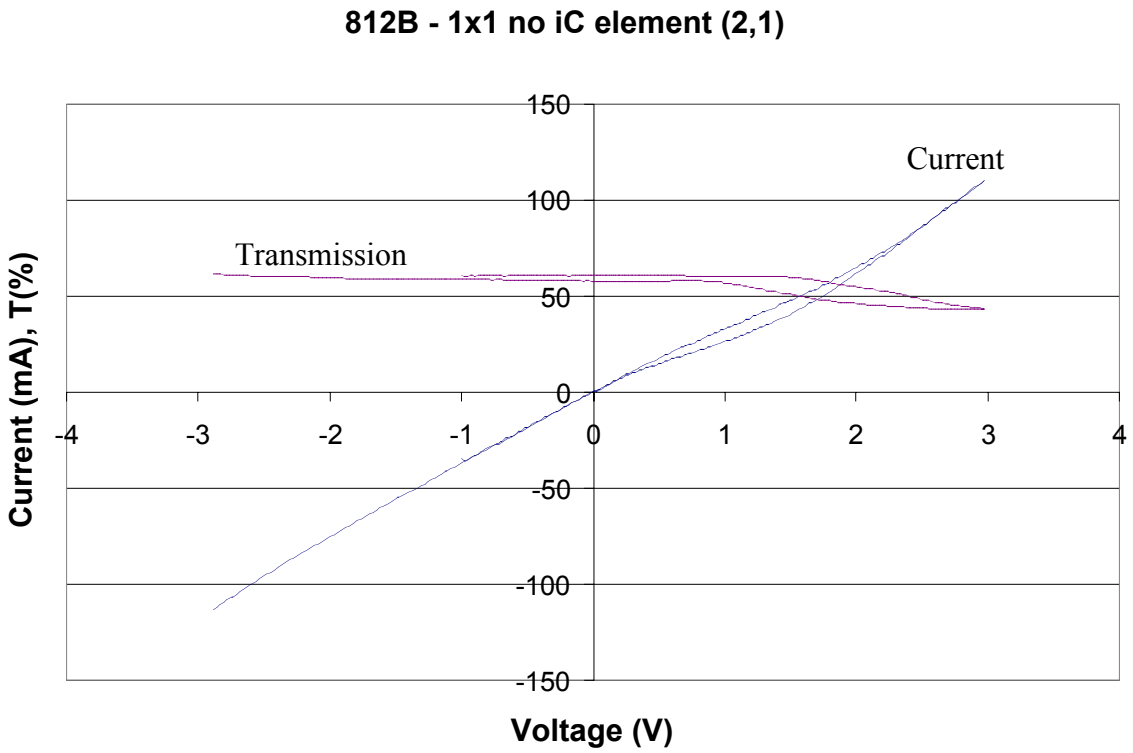

Figure III.9 – An example of a CV taken from an EC device made with no IC layer. Note the Ohmic behavior of the device, and poor coloration.

In contrast, three devices were made with a proprietary additive in the CE layer, again with no IC. The contrast in the electronic behavior is quite stunning, and is shown in Figure III.10 in the Appendix. These data are measured by setting a voltage and allowing the device to reach electrical equilibrium before recording the current.

Significant progress has been made in understanding the electronic behavior of the SageGlass® EC system. Our understanding is by no means complete, but we have gained a fundamental understanding of the critical process parameters, and this information has been fed into the pilot line. This requires that certain key process parameters are maintained within critical limits, and there has been a concomitant increase in the consistency and repeatability of devices produced by the pilot line. This is particularly evident in the care taken with the level of lithiation, as this is known to have a critical impact on the device behavior. Work continues in an effort to further understand the influence of changes made to the various layers (i.e. thickness, processing temperatures, etc.) on the electronic properties of the device.

IV. PROCESS IMPROVEMENT

IV.1 UTILIZE DOE TO OPTIMIZE FAB PROCESSES

Design of Experiments (DOE) is a planned approach for determining cause and effect relationships that can be applied to any process with measurable inputs and outputs. DOE provides a statistical means for analyzing how numerous variables interact. Designed experiments require some up front planning to be successful, as it is possible – even desirable – to study several different variables in one set of experimental runs. The generic name for this approach is "Factorial Design," and this will be briefly explained below. Coupled with the factorial design is the statistical analysis of variables (ANOVA), which allows dependencies and interactions between variables to be cleanly determined from the measured data.

The factorial design approach is in complete contrast to the more usual one factor at a time (OFAT) experimentation methodology, where only one factor is varied and all the others are held constant. In the factorial design approach, interactions between variables are revealed where they would be missed in the OFAT approach. In addition, the number of experimental runs required to investigate a certain volume of experimental space is reduced compared with OFAT, thus increasing the experimental power. The experimental power increases with an increase in the number of variable factors.

In general, we have limited ourselves to two-level factorial designs. Using this method, two levels (HIGH and LOW) are chosen for each variable factor. In a two-factor two-level design, there are therefore four unique combinations:

	Factor 1	Factor 2
1	HIGH	HIGH
2	HIGH	LOW
3	LOW	HIGH
4	LOW	LOW

Table IV.1 – Two-factor two-level design.

In a three-factor two-level factorial, there would be eight unique combinations of variables:

	Factor 1	Factor 2	Factor 3
1	HIGH	HIGH	HIGH
2	HIGH	HIGH	LOW
3	HIGH	LOW	HIGH
4	HIGH	LOW	LOW
5	LOW	HIGH	HIGH
6	LOW	HIGH	LOW
7	LOW	LOW	HIGH
8	LOW	LOW	LOW

Table IV.2 – Three-factor two-level design.

An experimental design would therefore run at least one sample with each combination, and the results from any measurements analyzed using the ANOVA approach. Naturally, the entire experiment can be replicated to give better statistical selectivity. Essentially, there would be four pairs of experimental points (1 and 5, 2 and 6, 3 and 7, and 4 and 8) which can be compared with each other where the only difference between the pairs is that (for instance) factor 1 is HIGH or LOW. If factor 1 is significant, then each of the pairs should show the same trend, so we have four experiments probing the significance of factor 1.

However, the factor could be involved in an interaction meaning that one factor depends on the value of another. As a trivial example of an interaction, we consider making scrambled eggs as our experiment, "cooking" as one variable factor (low level = no cooking, high level = cooked) and "mixing" as our second variable factor (low level = unmixed and high level = mixed) we can see that from our four combinations only one set will result in scrambled eggs. The ANOVA approach allows such interactions to be extracted from the measured data in a simple and clear way. Obviously, the effectiveness depends on the initial experimental design.

	Factor 1	Factor 2	Result
1	Uncooked	Unmixed	Raw eggs!
2	Uncooked	Mixed	Raw beaten eggs!
3	Cooked	Unmixed	Sunny side up or easy over
4	Cooked	Mixed	Scrambled eggs

Table IV.3 – Experimental design example.

An additional benefit of the DOE approach comes as the complexity of the system increases. As the number of variable factors increases, the number of unique combinations or experimental points goes up accordingly. However, we can actually run *fractional* factorial experiments without losing any statistical resolution where only a subset of the experimental combinations are required. For example, the table below shows the savings—meaning the number of redundant combinations – that can in principle be made by using fractional designs:

Number of Factors	Full Factorial	Fraction required	Savings
4	16	12	25%
5	32	16	50%
6	64	32	50%
7	128	32	75%

Table IV.4 – Fractional factorial designs.

The interested reader is referred to "DOE Simplified," by Anderson and Whitcombe (2000) Pub: Productivity Inc., or "Design and Analysis of Experiments," Montgomery, (1997), Pub.: Wiley, for further details on all aspects of DOE.

We have generally concentrated on full factorial designs, usually with two or three variable factors. The DOE methodology has been adopted completely, and is now used for process optimization experiments. The results of

several of these experiments are discussed in the section on the ion conductor studies (section II.3).

An example of an experiment that was run using the DOE methodology is shown in the Appendix. This illustrates the large amount of information that can be obtained from a simple experiment, and the dependencies of the measured data upon the experimentally varied factors.

IV.2 RAPID CONVENTIONAL HEATING

Much of the emphasis of the work in this area has been placed on thermal uniformity during the various heating processes. We have worked hard to minimize the variation seen across samples of various sizes during heat-up. This was necessary as we found that EC samples of different sizes—when heated in the same process run—would display different electrochromic behavior. We have found that this is due to the way that low-e glass samples that we use as our substrates heat differently depending upon which side is exposed to the heat source. This is because the low-e coating acts as a heat mirror, whereas the lamps used in this heater are designed to emit radiation that will be largely absorbed by the glass. It was found that with the samples placed coating side up (facing the lamps) in the oven, the coating reflected a high proportion of the incident radiation. However, a significant amount of heat was reflected off the bottom of the oven, leading to enhanced heating of the edges of the sample. This led to a significant edge to center variation of temperature for our samples and was more pronounced for the larger samples, leading us to reconsider the uniformity of our heating process.

The characterization of the uniformity was carried out by using a variety of sample sizes and orientations, gluing thermocouples in various positions to them, and running these samples through a thermal cycle. This gave us the uniformity for the various different sizes, and it was possible to minimize the variation by careful tuning of the temperature controller. As a result of this study, it was found that if we oriented the sample with the coating side down (away from the lamps), to maximize the amount of heat absorbed by the glass, and minimize the effect of the reflective low-e coating, we obtained much better uniformity. However, this caused the repeatability of the process to be compromised.

The repeatability of heating depends on the measurement of temperature used to control the power supplied to the oven. A pyrometer is used in our oven to look at the amount of heat radiating from the hot glass surface. The amount of heat emitted depends upon the emissivity (e) of the surface. This is very well defined for the glass surface (e=0.86), but can vary dramatically for the coated side depending on what coatings are present. In addition, the emissivity for the same sample can vary between room temperature and our typical processing temperatures, and so a single value (which is all that the pyrometer controller uses) cannot possibly describe the temperature accurately during the entire heating cycle.

We therefore decided to abandon the radiant heater in favor of a forced air convection oven. This has recently been installed, and the repeatability and uniformity have both significantly improved.

V. OPERATIONAL TESTING

V.1 DESIGN AND DEVELOP PROTOTYPE TEST STATION

Under this contract, a second large device tester was built with expanded capabilities for device characterization, and the software for both the existing and new testers was upgraded. An important objective was to develop the capability to test full size EC devices over a range of temperatures.

Temperature Control

The most significant hardware improvement was the addition of temperature control for the device under test. To accomplish this, a five-inch-deep thermally insulated enclosure was placed in front of the backlight, with air circulated through heating and/or cooling elements. For cooling, a liquid chiller cools a mixture of water and propylene glycol, which is circulated through an air/liquid heat exchanger. For heating, an electric heating element directly heats the air. A blower, used for both heating and cooling, circulates air through the insulated enclosure, heat exchanger, and heater.

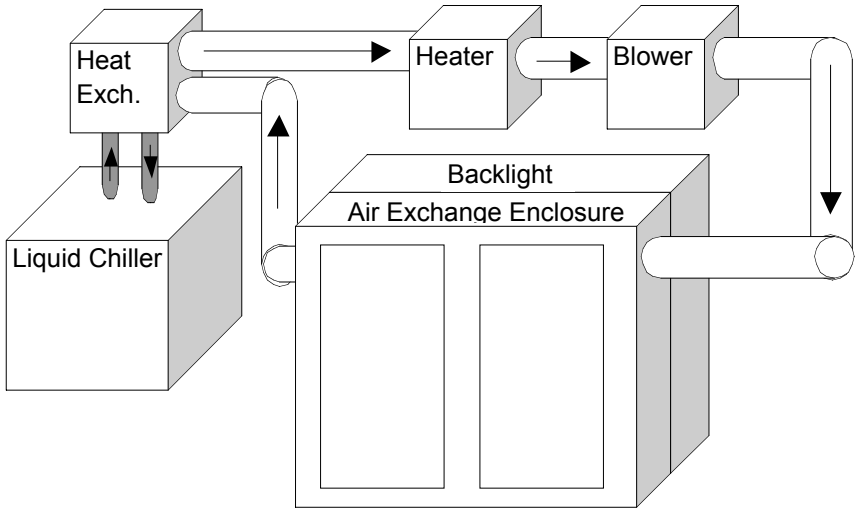

The electrochromic insulated glass units (IGUs) are placed in the front of the enclosure, with the active side toward the inside of the enclosure. In this way, the test system represents a somewhat realistic environment, with the active side “outdoors” (significant temperature range) and the inactive side “indoors” (consistent temperature.)

With this new system, it is possible to thoroughly test various IGU sizes over a temperature range from below 15°C to at least 65°C. While this temperature range is more limited than actual field conditions, it is sufficient to allow development of a device model that incorporates temperature effects. Without this piece of equipment, this would have been nearly impossible, as previous test systems with temperature control were inside environmental-control chambers, allowing only a couple of spot-measurements of light transmission via fiber optics. Spot measurements, while helpful in some contexts, do not provide enough information to accurately develop a device model.

Another helpful application of this test system is its ability to show device kinetic performance over a range of temperatures. Some non-uniformity in EC devices is temperature-dependent, making it hard to fully understand the effect on user perception without this sort of test system.

Test Sequencing

The sequencing of tests has also been significantly improved, allowing more rapid, efficient testing of electrochromic devices. The figure to the right shows the dialog box used to set up individual and sequential tests.

The "Mode Select" element in the upper-left corner of the image is used to select an automatic, manual, sequenced, or looped test. Automatic and manual tests have always been available. Manual tests simply log data while allowing the operator full control of applied voltage and transmission limits. Automatic tests apply a sequence of voltages, voltage ramps, or transmission limits.

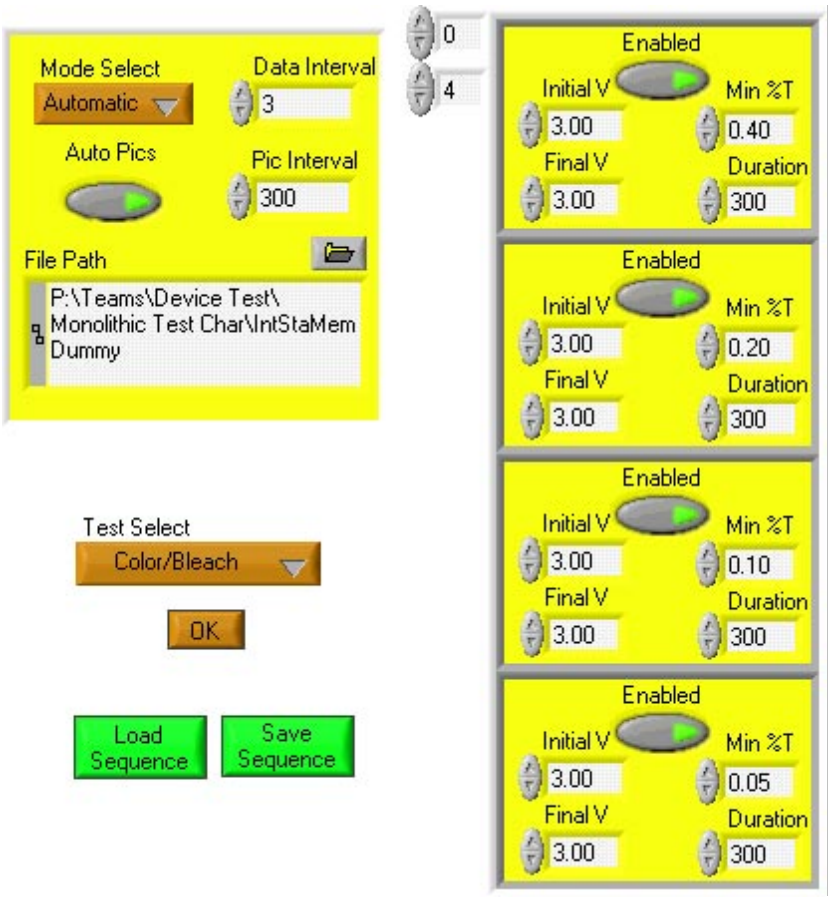

Figure V.1 – Test dialog box.

The new "sequential" mode allows the operator to set up a series of discrete tests, performed in sequence, saving the data to separate files, as shown in the "File Path" box, and as many as five sequential tests may be run.

The "looped" test simply runs a sequence of operations over and over until interrupted by the operator. This could be used, for example, to alternately color and bleach a device, holding it for a specified period of time in each state. This has been used, for example, to investigate device properties which seem to change during the first few cycles. Finally, any test which is set up by the operator may be saved as a script file (using the "Load Sequence" and "Save Sequence" buttons shown in the lower left corner of the dialog box.) In this way, an operator may create a test sequence that is used repeatedly with a minimum of set-up work.

V.2 ELECTRO-OPTICAL DEVICE MODEL

Introduction

The objective of this work is to determine a set of fundamental device parameters that can be used to describe all the key performance parameters of an EC device. These parameters would be most useful if they could be determined from a simple characterization test. Another potential use would also be to use these parameters to distinguish devices that are likely to degrade over time. Successfully achieving these objectives would dramatically reduce the amount of testing and characterization required, help in developing control algorithms and reduce potential degradation of samples in the field.

To accomplish these objectives, it is necessary to develop an understanding of the electro-optical properties, yielding a parameterized model. This model would be required to describe the behavior of EC devices as a function of temperature as well as the room temperature response. Our work has so far focused on developing and refining an equivalent circuit model based on standard electrical circuit elements. We are also developing an understanding of the solid-state physics and electrochemistry of the device – discussed in Section III.1 – which will help to illuminate the dependence of our circuit element model on physical properties of the EC devices.

Initially, we consider the behavior of EC devices at constant temperature. Two important relationships can be derived from measurements of SageGlass® windows at equilibrium (that is, under conditions of steady-state voltage, current, and transmission). These are the relationship of voltage to electronic current (at equilibrium there is no ionic current) and the relationship of voltage to transmission state.

Transmission state, in this document, will be given in units of optical density. Voltage will be given as "*internal voltage*," which is an approximate measurement of the voltage applied to the electrochromic stack; that is, the applied voltage less the voltage drop across the transparent conductors and bus bars. The purpose of using "internal voltage" is to minimize the size-dependence of the measurements.

Detailed measurements of optical density and current as a function of internal voltage for actual EC devices are presented in the Appendix.

Theoretical Understanding

The following is a discussion of our current understanding of the theoretical principles concerning the parameters discussed in previous sections. Figure V.2 below shows a schematic (model equivalent circuit) for the EC device which we have deduced from our studies of the electronic behavior of EC devices. This represents a single element of the device, and in order to explain the behavior of a large area device, this could form the basis for one spatial element of a finite element model.

Essentially, the model can be split into two parts: an electronic pathway and an ionic pathway. The measured current will be the sum of these two components, and the main challenge in understanding (and hence the ability to control the device) is in disentangling the two components.

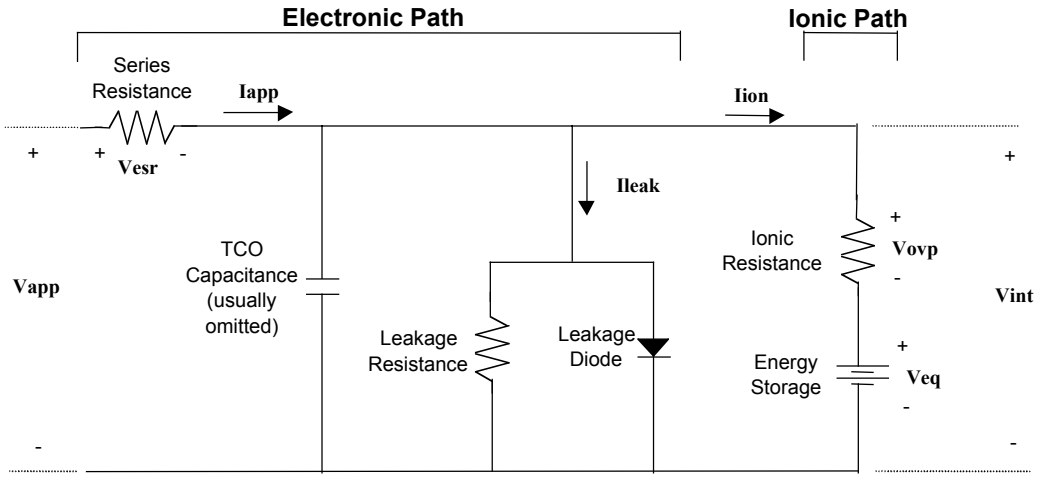

Figure V.2 – Device schematic model (equivalent circuit).

The applied voltage (V_{app}) causes a current (I_{app}) to flow into the device through the series resistance (primarily made up of the transparent conductor sheet resistances and the bus bars). This current then is split into the ionic and electronic components. We have found that the electronic current (I_{leak}) follows a path that appears electronically to be equivalent to a diode in parallel with a resistor.[9] The ionic path appears to be equivalent to a resistance in series with a charge storage element. The following sections describe some characteristics of the equivalent circuit in more detail.

Breakdown Voltage

The "breakdown" behavior (associated with the leakage diode in the electronic pathway) appears to be a property of the junction between the CE and the WO_3. We expect the breakdown behavior to be dependent on the material properties of the WO_3, IC and CE layers, and on the interfaces between them. We note, however, that varying the thickness of the layers does not appear to significantly change the breakdown voltage, and that the behavior is asymmetric (different for coloring and bleaching potentials).

Voltage Efficiency

Voltage efficiency (change in optical density per voltage increment) seems to be, in large part, a measure of the

[9] It is possible to increase the sophistication of the model by including two such circuit elements, with two diodes oriented in opposite directions with different breakdown voltages, reflecting the different breakdown voltages seen in the forward and reverse directions.

"battery capacity" of the EC stack. Consider, for example, the difference between a C and D cell. More charge is required to charge a D cell to a given voltage because of its large capacity. Replace "charge" with "optical density" in that sentence and one can see that a D cell has a higher voltage efficiency (more charge per volt). We have seen this in some experiments where we have made devices with 2 and 6 passes of CE, rather than our more typical 4. Devices with 2 passes of CE had voltage efficiencies less than 0.5. Those with 6 passes were generally between 1.2 and 1.5. It is also probable that lithiation affects voltage efficiency. Again, this is not surprising, since the "battery capacity" is a function of WO_3, CE, and lithium. It appears that, at the moment, CE is more of a limiting factor for coloration than WO_3, so variations in CE have more effect on voltage efficiency. Leakage variations also appear to have some effect on this measurement, though this is not well established or quantified.

Threshold Voltage

The threshold voltage (voltage required to begin coloring a device) is a function of electrochemical potential of the WO_3 and CE, which can be affected by the amount of incorporated lithium, and probably deposition conditions and heating of the various layers (during and after deposition). We have very little hard data at the moment to extract much meaning from this parameter, except to note that lower thresholds are better from a performance standpoint.

Leakage Resistance

Leakage resistance appears to be dominated by defects—devices without shorts have a very high leakage resistance, which is to say very low electronic current at voltages below breakdown. It has been speculated that all leakage is a matter of defects—perhaps micro-defects which aren't visible. It is clear that the potential for very low leakage current is achievable with our present stack— samples with dimensions 19"x37" have been observed holding at 5% transmission drawing less than 20 mA current at less than 1.5V potential.

SUMMARY

Significant progress has been made in our understanding of the electro-optical behavior of EC devices. Indeed, we have invented several terms to describe the behavior we have observed. Our lumped parameter model is fairly well established, although we have identified areas where the level of sophistication can be increased. We already use at least one of the parameters (the series resistance) in monitoring the evolution of the device performance as it undergoes durability testing. This measurement is simple, and can be used to determine whether the physical integrity of the device has been compromised without the need to perform a full color-bleach characterization.

Future work will focus on the detailed understanding of the model, and the relationship of variations in the EC film deposition process to elements within this parameterized model. In addition, the temperature dependence of EC devices will be studied in more detail, and the consequences for design of practical controllers and control algorithms determined.

IGU DURABILITY AND INTEGRITY

VI.1 OPTIMUM ELECTRICAL CONNECTION

Sage has developed a proprietary low cost feedthrough system which is describe in Section VI.1.1 in the Appendix.

VI.1.2 Durability tests on low cost feedthrough system

Industry standard IGU seal tests have been carried out in order to determine the integrity of the low cost electrical feedthrough. An argon diffusion test was carried out to determine the diffusion rate of the argon filler gas through the feedthroughs and sealing materials. The requirement for passing the argon retention test is less than 1% diffusion from the IGU per year. SAGE IGUs with the under the low cost feedthrough showed an average annual diffusion of 0.71%. Samples with this IGU configuration also passed the P1 test, a French (soon to be European) standard weathering test, and a European humidity test (test specifics detailed below). These results have indicated that this low cost feedthrough approach is durable to water ingress and does not accelerate argon diffusion compared to standard insulating glass units.

VI.2 DEVELOP TESTS TO ENSURE IGU DURABILITY

Accelerated weathering and seal testing

During the course of this project, we have developed a testing program in which IGUs with the SAGE sealing system and full SageGlass® IGUs (fully operational units) have been subjected to industry standard tests, modifications of these standard tests and new tests. The test modifications have been designed to better stress this new IGU product. The key issues this test program is aimed to address are as follows:

- Integrity of the IGU sealing system with respect to water ingression into the air gap – does the feedthrough present a path for water?
- Integrity of the IGU sealing system with respect to argon retention
- Quality of SAGE's fabrication process
- Durability of the solder joint which is external to the spacer with respect to corrosion

This testing program has been implemented with help from our customers and partners and the program of tests that have been used and developed for our durability evaluations, are:

- P1 test (constant UV irradiation at the seals and water spray at 60 °C)
- The French IGU weathering test (includes thermal cycling, relative humidity and UV radiation) which will soon become the European standard
- European argon retention test
- The European humidity test
- A customer's weathering test (UV, thermal cycling, one edge of IGU in water, humidity)
- More stringent, modified, version of US ASTM humidity test (developed in-house)
- Salt fog test (developed in-house)

Test results

Argon retention test – This test was carried out for us by a customer-partner and the results are discussed above in Section VI.1.2.

P1 test – The P1 test is used routinely by Cardinal, the leading fabricator of IGUs, and is believed by Cardinal to be the most stringent weathering test, more so than the ASTM weathering test (ASTM 774). Cardinal has found a 1-week-in-test to 1-year-in-the-field correlation to lifetime and set the pass requirement in this test at 40 weeks. Initially, we tested units with the SAGE feedthrough system with and without SageGlass® films, which successfully surpassed the 40 week requirement. These results indicate the durability of the SAGE sealing system and SAGE's fabrication quality. Next, to test the corrosion durability of the electrical connections (wire-solder joint-bus bar) outside the primary seal, full SageGlass® IGUs were electrochromically cycled (to ensure the connections have an electrical potential across them) while under the P1 stress. Five of five units survived 58 weeks in the test while accruing approximately 30,000 EC cycles. All are fully operational as EC devices, pass the dewpoint requirements indicating no seal failure, and the electrical connections show no sign of performance degradation.

European tests – The French weathering test: European humidity test, and customer's weathering tests have been carried out on IGUs with the SAGE feedthrough and sealing system by a customer-partner. The positive results support the indications from P1 test results that both the sealing system and SAGE's fabrication quality are good.

We have also constructed an IGU tester in which the window is tested in 100% relative humidity with one edge in liquid water.

Modified humidity test – We have designed and built a humidity test in-house which we feel is a more stringent version of the ASTM humidity test for IGUs, which increases the test temperature from 60° to 75°C and has one edge of the IGU immersed in water while the remaining atmosphere is close to 100% relative humidity. Depending on the test, the end of the IGU with the electrical connections can be immersed in the water. In addition to the environmental stresses, the electrical connections are further stressed by continually cycling the devices from clear to dark to clear. To date, 22 units have undergone eight months of EC cycling with contacts in water, 16 of which continue to exhibit no change in electrical system performance (no impact of corrosion). The other six samples exhibited seal failures due to the humidity stress. It should be noted that the ASTM standard humidity test requires units to survive only 14 days in 95% RH and 60^{o}C.

Salt Fog – We have also initiated an even more highly accelerated test—using a salt fog chamber—to investigate the potential for corrosion of the EC electrical connections, which are located outside the air gap, under the secondary seal. In this test, just as with the P1 and in-house humidity test, the SageGlass® IGUs are electrochromically switched while exposed to highly concentrated salt water (5 times that of sea water) at 40^{o}C. The resistances of the electrical connections are being monitored as a function of time, to monitor any loss of electrical performance due to corrosion. After four months in the test, seven of the original 10 devices are still operational

without electrical system failure. Three devices failed because silicone secondary seal coverage was not sufficient around the spacer—salt attacked the aluminum spacer causing a hole and loss of desiccation inside the IGU.

Summary

The above results continue to indicate that there are minimal issues associated with corrosion of the electrical connections in the SageGlass® IGU configuration as long as the solder joints are covered completely with silicone. At this point in the test program implementation, the electrical configuration and IGU seal looks durable to the expected environmental stresses.

VI.3.1 Impact of thermal shock on EC IGUs

When a SageGlass® IGU is in its dark state under direct sun, it absorbs significant heat and consequently gets very hot. If a sudden rain storm occurred, the water would cause the glazing to cool very rapidly (a thermal shock). Also, if the glazing is very cold, (e.g. during the winter in northern climates), and the glazing comes suddenly under direct sun, in its darkest state it will absorb energy and its temperature will rise rapidly, again resulting in thermal shock. Even commercially available tinted glazings in use today have visible light transmissions significantly higher than that of the dark state of SageGlass® glazings so the rate of change of temperature of these glazings under the same conditions is likely to be significantly less. Clearly, not only will thermal shocks cause stress to the coatings, they will also stress the film to bus bar connections and the IGU sealing system itself. To evaluate the durability of the SageGlass® IGU system to thermal shocks, SAGE has developed a test system that simulates and exaggerates the thermal shocks that a window would experience in the actual environment. Briefly, the SageGlass® IGU is mounted in a metal frame directly in front of an array of solar simulating lamps. The test is located outside, so that the temperature of the glazing varies with the outside ambient temperature. In a given transmission state, the window can be suddenly illuminated by irradiation of intensity greater than 1 sun (AM 1.5). An automatic shower can be triggered to simulate the thermal shock of rain. Masks can also be placed over portions of the glazing to simulate partial shading. Thermocouples are placed over the front and back surfaces of the glazing to measure temperature gradients.

Over the course of 15 months, one SageGlass® IGU survived more than 3,000 thermal shocks, 770 of which included rapid cooling, without seal failure or EC failure. The largest cooling rates measured were 140°C/minute, with a 56°C temperature difference between the front and back lite. In order to make the test a better representation of a real environment the test has been modified so that the glazing is now glazed into an air conditioned box, which keeps the inside lite of the IGU at a constant room temperature (as it would be in a real installation) while the outside EC lite is illuminated. Temperature gradients and cooling and heating rates have been observed to be significantly reduced as a result of this modification, indicating that the original test was indeed very highly accelerated.

VII. RELIABILITY

VII.1.1 Design Comparison Experiment:

We are exploring the relationship between the PI test and life of dual pane windows in the field. One of the partners in this project has collected significant data on field failures. Another accelerated test that is being considered for predicting product life in the field is the ASTM Standard Test Method for Assessing the Durability of Electrochromic Coatings in IG Units.